Elsevier Editorial System(tm) for Environmental and Experimental Botany
Manuscript Draft

Manuscript Number:

Title: Changes induced by cadmium stress and iron deficiency in the composition and organization of thylakoid complexes in sugar beet (Beta vulgaris L.)

Article Type: Research Paper

Keywords: sugarbeet; Cd stress; Fe deficiency; thylakoids; Blue-Native PAGE

Corresponding Author: Ms. Brigitta Basa,

Corresponding Author's Institution:

First Author: Brigitta Basa

Order of Authors: Brigitta Basa; Giuseppe Lattanzio; Ádám Solti, Ph.D.; Brigitta Tóth; Javier Abadía, Ph.D.; Ferenc Fodor, Ph.D.; Éva Sárvári, Ph.D.

Abstract: In intact plants, Cd-induced Fe deficiency is thought to play a role in the toxic effects of Cd on photosynthesis. To investigate the contribution of the Cd-induced Fe deficiency to Cd stress symptoms we studied the composition and organization changes of thylakoid pigment-protein complexes by two-dimensional Blue Native-SDS gel electrophoresis and mass spectrometry, in parallel to functional changes, using Beta vulgaris plants grown in hydroponics. Plants were treated by withdrawing of Fe or with 10 μM CdCl2 for 10 days. Both metal stresses caused a marked decline in leaf chlorophyll concentration and chloroplast Fe content, as well as a loss in photosystem I (PSI) and light harvesting complex II (LHCII) particles. Furthermore, organizational changes of the photosynthetic apparatus were found, including a decrease in the ratio of the PSII mega-/supercomplexes and an increase in the monomeric form of the LHCII antennae, with the extent of these changes being similar under both stresses. This supports that Fe deficiency responses have a major role in the responses of plants under Cd stress. In the Fe-deficient thylakoids, an increase in the ratio of PSI supercomplexes and degrading PSII particles was more pronounced, together with a higher zeaxanthin content. Under Cd stress, a stronger inhibition of PSII activity and enhancement of thermal dissipation of the inactive PSII complexes were observed. The differences detected under the two metal stresses lead to the conclusion that both local Fe deficiency in chloroplasts and other direct or indirect inhibitory effects of Cd are behind the response mechanisms of plants grown under Cd stress.

EÖTVÖS LORÁND UNIVERSITY
INSTITUTE OF BIOLOGY
DEPARTMENT OF PLANT PHYSIOLOGY AND MOLECULAR PLANT BIOLOGY
✉ **H-1117 Budapest, Pázmány Péter Lane 1/C.**
Tel.: +36 1 381 2163 Fax: +36 1 381 2164

7th of November 2013

Dear Kari Taulavuori,

Here, as the corresponding author, I am sending our manuscript authored by Basa *et al.*, titled '**Changes induced by cadmium stress and iron deficiency in the composition and organization of thylakoid complexes in sugar beet (*Beta vulgaris* L.)**' intended to publish in Experimental and Environmental Botany.

This manuscript represents an original work that is not being considered for publication, in whole or in part, in another journal, book, conference proceedings, or government publication with a substantial circulation.

All of the authors have contributed substantially to the manuscript and approved the final submission.

Physiological changes of plants under Cd stress are widely studied, and many of the symptoms are associated to a Cd-induced Fe deficiency. In Cd-stressed plants, inhibition of Chl synthesis and decrease in photosynthetic activity occurs together with decreased accumulation and reorganization of the pigment-protein complexes of thylakoids. Our paper addresses the question **in what extent is responsible the Cd-induced Fe deficiency for these acclimation responses of thylakoids under Cd toxicity.** In order to study the amount of the different membrane complexes and their interactions Blue Native/ SDS-PAGE method combined with mass spectrometry protein identification was used to characterize the proteome profile of thylakoids of both Cd-stressed and Fe-deficient sugar beet plants along with parallel fluorescence induction studies on functional changes.

The key points of our finding are:

- Cd-induced local Fe deficiency in the chloroplast is the prime trigger of thylakoid acclimation.
- Both Cd stress and Fe deficiency induce the accumulation of PSII supercomplexes and at the same time the disassembly of LHCII.

- Increased intensity of cyclic electron flow and accumulation of zeaxanthin, the main quenchers under severe Fe depletion, seems not to take part in the protective mechanisms under Cd stress but rather thermal dissipation by inactive PSII complexes.

Our results appreciably contribute to the sparse structural information on thylakoid complexes affected by Cd toxicity and Fe deficiency.

All previously published work cited in the manuscript has been fully acknowledged.

I am looking forward to hearing from you at your earliest convenience.

With best regards,

Yours faithfully,

Brigitta Basa

Highlights:

- Cd-induced chloroplast Fe deficiency is a prime trigger for thylakoid acclimation to Cd excess.
- Both Cd stress and Fe deficiency induce PSII supercomplex and LHCII disassembly.
- Thermal dissipation by inactive PSII complexes is markedly induced by Cd stress.
- The amounts of PSI supercomplexes and zeaxanthin rise with Fe deficiency.
- Cyclic electron flow and zeaxanthin are likely to be energy quenchers under low Fe.

Changes induced by cadmium stress and iron deficiency in the composition and organization of thylakoid complexes in sugar beet (*Beta vulgaris* L.)

Brigitta Basa[a*1], Giuseppe Lattanzio[b], Ádám Solti[a], Brigitta Tóth[c], Javier Abadía[b], Ferenc Fodor[a], Éva Sárvári[a]

[a] Department of Plant Physiology and Molecular Plant Biology, Eötvös University, Pázmány P. lane 1/C, Budapest H-1117, Hungary

[b] Department of Plant Nutrition, Aula Dei Experimental Station (CSIC), P.O. Box 13034, E-50080, Zaragoza, Spain

[c] Department of Agricultural Botany and Crop Physiology, Institute of Crop Sciences, Centre for Agricultural and Applied Economic Sciences, University of Debrecen, Böszörményi street 138. Debrecen, H-4032 Hungary

***Corresponding author:**

Brigitta Basa

e-mail: basa.brigitta@gmail.com

[1] Current address: 17310, Pg. Buenos Aires 20, 1/M, Lloret de Mar (Girona, Spain)

e-mail addresses:

Giuseppe Lattanzio: giuseppe.lattanzio@eead.csic.es

Ádám Solti: sadambio@elte.hu

Brigitta Tóth: btoth@agr.unideb.hu

Javier Abadía: jabadia@eead.csic.es

Ferenc Fodor: ffodor@ludens.elte.hu

Éva Sárvári: e_sarvari@ludens.elte.hu

Abstract

In intact plants, Cd-induced Fe deficiency is thought to play a role in the toxic effects of Cd on photosynthesis. To investigate the contribution of the Cd-induced Fe deficiency to Cd stress symptoms we studied the composition and organization changes of thylakoid pigment-protein complexes by two-dimensional Blue Native-SDS gel electrophoresis and mass spectrometry, in parallel to functional changes, using *Beta vulgaris* plants grown in hydroponics. Plants were treated by withdrawing Fe or with 10 µM $CdCl_2$ for 10 days. Both metal stresses caused a marked decline in leaf chlorophyll concentration and chloroplast Fe content, as well as a loss of photosystem I (PSI) and light harvesting complex II (LHCII) complexes. Furthermore, marked organizational changes of the photosynthetic apparatus were found, including a decrease in the ratio of the PSII mega-/supercomplexes and an increase in the monomeric form of the LHCII antennae, with the extent of these changes being similar under both stresses. This supports that Fe deficiency responses have a major role in the responses of plants under Cd stress. In Fe-deficient thylakoids the increase in the ratio of PSI supercomplexes and degrading PSII particles was more pronounced, and a higher zeaxanthin content was found. Under Cd stress, a stronger inhibition of PSII activity and enhancement of thermal dissipation of the inactive PSII complexes were observed. The differences detected under the two metal stresses lead to the conclusion that both local Fe deficiency in chloroplasts and other direct or indirect inhibitory effects of Cd are behind the response mechanisms of plants grown under Cd stress.

Keywords: sugar beet; Cd stress; Fe deficiency; thylakoids; Blue-Native PAGE

Abbreviations: BN: blue-native; CA: connecting antenna; Chl: chlorophyll; FNR: ferredoxin-$NADP^+$ oxidoreductase; LHC: light-harvesting complex; NPQ: non-photochemical

quenching; PAGE: polyacrylamide gel electrophoresis; PS: photosystem; SDS: sodium-dodecyl-sulfate; VAZ: violaxanthin+antheraxanthin+zeaxanthin

1. Introduction

Cadmium (Cd) is a heavy metal pollutant that is dangerous to all living organisms. In nature, Cd can be released as a result of rock mineralization processes, but the main sources of contamination are anthropogenic activities, including urban traffic, cement factories, metal-working industries, waste incinerators, and the use of P fertilizers or sewage sludge manures (Nagajyoti et al., 2010). Cadmium is well known for its phytotoxicity, and therefore its accumulation in soils leads to reduced yields in horticultural and forest crops by altering many plant physiological and biochemical processes (Sanità di Toppi and Gabbrielli, 1999). Although the total amount of Cd taken up by plants is largely species-specific, Cd toxicity usually causes similar symptoms in most species, such as reduced growth, decrease in photosynthesis and disturbances in ion uptake (Prasad, 1995; DalCorso et al., 2008).

Damages of the photosynthetic apparatus are related to different direct and indirect mechanisms induced by Cd. As a consequence of its capacity to replace essential metals in metal binding proteins, Cd can induce inhibition of chlorophyll (Chl) synthesis and also disturb PSII function (Bertrand and Poirier 2005; Faller et al., 2005; Kučera et al., 2008). A direct inhibition of O_2 evolution by Cd is also possible (Sigfridson et al., 2004; Pagliano et al., 2006). Because of its stable binding to -SH groups of proteins, Cd may interfere directly with enzymes related to Chl biosynthesis (Stobart et al., 1985; Padmaja et al., 1990) and C assimilation (van Assche and Clijsters, 1990), and also with the correct assembly of the pigment-protein complexes of both photosystems (Baryla et al., 2001). As a secondary effect, the oxidative stress induced by Cd can lead to an imbalance in the generation and removal of

72 reactive oxygen species capable of damaging membranes, proteins and nucleic acids (Kučera
73 et al., 2008).

74 In intact plants, many of the symptoms of Cd stress are associated to a Cd-induced Fe
75 deficiency (Siedlecka and Krupa, 1999; Larbi et al., 2002; López-Millán et al., 2009).
76 Cadmium inhibits the root Fe(III) reductase (Alcántara et al., 1994; Chang et al., 2003) and
77 impairs Fe uptake and translocation of Fe from roots to shoot (Fodor et al., 2005), leading to
78 Fe deficiency in leaves. Iron deficiency itself is also a serious worldwide problem in
79 numerous crops (Marschner, 1995). In chloroplasts, Fe plays important roles in Chl synthesis
80 (Spiller et al., 1982; Tanaka et al., 1998), and photosynthesis, which utilizes heme- and Fe-S
81 proteins, is also markedly affected by Fe deficiency (Belkhodja et al., 1998; Larbi et al.,
82 2006). Changes in Chl fluorescence parameters and loss and recovery of photosynthetic
83 components found under Cd stress showed a strong correlation with the Fe status of the
84 nutrient media (Solti et al 2008; Qureshi et al., 2010), underscoring the importance of Fe
85 deprivation induced by Cd on photosynthetic processes.

86 Both the inhibition of Chl synthesis and the reduced photosynthetic activity are associated
87 not only to a decreased accumulation, but also to a reorganization of pigment-protein
88 complexes. The accumulation of PSI was strongly reduced under Cd exposure (Sárvári et al.,
89 1999, 2005; Fagioni et al., 2009, Qureshi et al., 2010), and a decreased amount of some
90 members of the Lhc family was also described in proteomic studies investigating Cd stress
91 (Kieffer et al., 2009; Farinati et al., 2009; Durand et al., 2010). Regarding Fe deficiency, a
92 high sensitivity of PSI and LHCII complexes was found (Andaluz et al., 2006; Timperio et
93 al., 2007). Not much information has been published concerning the organizational changes
94 of thylakoid complexes induced by Cd or Fe deficiency, although the oligomerization of
95 LHCII has been shown to be disturbed by both stresses in different plant species (Krupa,
96 1988; Timperio et al., 2007; Fagioni et al., 2009; Qureshi et al., 2010; Saito et al., 2010).

Interactions between thylakoid pigment-protein complexes play important roles in protective mechanisms, especially under stress conditions that lead to imbalances between the absorbed and utilised light energy. When light is in excess, antenna associated quenching mechanisms are activated, including the so-called non-photochemical quenching (NPQ) processes that involve dynamic changes in the organization of the antennae (Li et al., 2002; Miloslavina et al., 2008; Betterle et al., 2009; Nilkens et al., 2010). Under strong stress conditions, these protective mechanisms can be insufficient, leading to inactivation of PSII centres associated with the controlled degradation and re-synthesis of the D1 (and D2) proteins of PSII centre (Andersson and Aro, 2001). For instance, in Indian mustard plants the Cd-induced decrease in the accumulation of multimeric complexes was attributed to an accelerated turnover of PSII (Qureshi et al., 2010). The long-term consequences of the imbalance in the activity of the two photosystems include changes in the gene expression, generally leading to an altered ratio and organization of the core and antenna components (Wilson et al., 2006). Iron deficiency was also shown to cause remodelling of the photosynthetic apparatus (Morales et al., 2001; Moseley et al., 2002; Saito et al., 2010).

In this study we aimed to compare the effects of Cd toxicity and Fe deficiency on the organization and functioning of thylakoid complexes, to better understand the impact of Fe deficiency itself and its contribution to Cd toxicity symptoms. In order to characterize the proteome profile of thylakoids, Blue Native (BN)-sodium dodecyl sulfate-polyacrylamide gel electrophoresis (SDS-PAGE) was used, together with mass spectrometry protein identification, to provide quantitative information on the amount of membrane complexes and also on their interactions.

2. Materials and Methods

2.1 Plant material

Hydroponically cultured sugar beet (*Beta vulgaris* cv. Orbis) plants were used. Seeds were germinated and grown in vermiculite for 2 weeks. Seedlings were grown in a climate chamber (16/8 h light [350 µmol m^{-2} s^{-1} PPFD PAR]/dark periods, 23/18 °C and 80% relative humidity) in 1/2 strength Hoagland solution: (in mM) 2.5 $Ca(NO_3)_2$, 2.5 KNO_3, 1.0 $MgSO_4$, 0.5 KH_2PO_4, 0.5 NaCl, (and in µM) 23.12 H_3BO_3, 9.2 $MnCl_2$, 0.28 $ZnSO_4$, 0.24 Na_2MoO_4, 0.16 $CuSO_4$, with 45 µM Fe(III)-EDTA. Before treatments, seedlings were pre-cultivated in nutrient solution up to four-leaf stage in plastic buckets of 20 L volume (4 plants per bucket), and then further cultivated in the above-mentioned nutrient solution (control) or treated with 10 µM $CdCl_2$ (+Cd), or by Fe deprivation (zero Fe and 1 g L^{-1} $CaCO_3$; -Fe) for 10 days. Nutrient solutions were changed weekly, and young, fully expanded leaves were sampled from the plants submitted to the differently treatments.

2.2 Determination of elemental content

All plant tissues were washed with ultrapure water. Samples were dried in an oven at 60 °C for 76 h until constant weight. Dried plant materials were digested with HNO_3 for 30 min at 60°C, then in H_2O_2 for 90 min at 120°C. Ion contents were measured by ICP-MS (Inductively Coupled Plasma Mass Spectrometer, Thermo-Fisher, USA) for microelements and by ICP-OES (Inductively Coupled Plasma Optical Emission Spectrometer, Perkin-Elmer, USA) for macroelements, using 3 replicates per treatment (n=3), each pooling leaves from four different plants. Chloroplast Fe content was determined according to Solti et al. (2012).

2.3 Determination of photosynthetic pigments

Leaf disks were cut with a calibrated cork borer, wrapped in aluminium foil, frozen in liquid-N_2, and stored at -80 °C for both Chl and carotenoid analysis. Leaf pigments were extracted with 80% (v/v) acetone in the presence of Na-ascorbate, and Chls were measured spectrophotometrically using the extinction coefficients of Porra et al. (1989). Pigment

extracts were filtered through OlimPeak 0.45 µm filters (Teknokrama, San Cugat del Vallés, Spain) and analysed in a Waters HPLC by the method described in Larbi et al. (2004). A flow rate of 1.7 mL min^{-1} was used, and the analysis time per sample was approximately 15 min including column equilibration. Pigments were detected at 450 nm using a photodiode array detector (Waters 996, Waters Corporation) and quantified by integration of peak areas. Three replicates per treatment were used.

To extract pigments from the main complexes obtained by BN PAGE, gel bands were excised with a surgical blade and the gel matrix was broken with a teflon homogenizer in the presence of 2 mM Tris-maleate (pH 7.0). In order to obtain an efficient recovery of the complexes, samples were stored overnight at -20 °C and then centrifuged at 12,000 g for 10 min. Supernatants containing the extracted chlorophyll-protein complexes were concentrated with Centricon 10.000 MWCO devices (RCYM-10, Millipore, Billerica, MA, USA) at 6,500 g until 300-500 µl final volume and filtered with OlimPeak 0.2 µm Syringe filters (Teknokroma, Barcelona, Spain). Separation cartridges (Sep-Pak Plus C_{18} Plus Short cartridges WAT020515; Waters Corporation, Milford, MA, USA) were first equilibrated with 100% (v/v) methanol and then with 4:1 methanol:water mixture. Then, samples were loaded in aqueous phase onto the cartridge and two mL of pure methanol was injected subsequently to remove non-adsorbed compounds (this procedure did not cause the elution of pigments from the column). Elution of the pigments was carried out using five mL of pure acetone, and analysis was carried out by HPLC as indicated above.

2.4. Photosynthetic activity measurements, quenching analysis

Fluorescence induction measurements were carried out with intact leaves using a PAM 101-102-103 Chlorophyll Fluorometer (Walz, Effeltrich, Germany). Leaves were dark-adapted for 30 min. The F_0 level of fluorescence was determined by switching on the measuring light

(modulation frequency of 1.6 kHz and photosynthetic photon flux density (PPFD) less than 1 µmol m^{-2} s^{-1}) after 3 s illumination with far-red light in order to eliminate reduced electron carriers (Belkhodja et al., 1998). The maximum fluorescence yields, F_m in the dark-adapted state and F_m' in light-adapted state, were measured by applying a 0.7 s pulse of white light (PPFD of 3500 µmol m^{-2} s^{-1}, light source: KL 1500 electronic, Schott, Mainz, Germany). The maximal and actual efficiency of PSII centres were determined as $F_v/F_m = (F_m - F_0)/F_m$ and $\Delta F/F_m' = (F_m' - F_t)/F_m'$, respectively. For quenching analysis, actinic white light (PPFD of 100 µmol m^{-2} s^{-1}, KL 1500 electronic) was provided. Simultaneously with the onset of actinic light the modulation frequency was switched to 100 kHz. The steady-state fluorescence of light-adapted state (F_t) was determined when no change was found in F_m' values between two white light flashes separated by 100 s. For assessing the excitation energy allocation in all samples, the quenching parameters of Hendrickson et al. (2005) were used as follows:

$$\Phi_{PSII} = \left(1 - \frac{F_t}{F_m'}\right) * \left(\frac{F_v / F_m}{F_{vM} / F_{mM}}\right);$$

$$\Phi_{NPQ} = \left(\frac{F_t}{F_m'} - \frac{F_t}{F_m}\right) * \left(\frac{F_v / F_m}{F_{vM} / F_{mM}}\right);$$

$$\Phi_{f,D} = \frac{F_t}{F_m} * \left(\frac{F_v / F_m}{F_{vM} / F_{mM}}\right);$$

$$\Phi_{NF} = 1 - \frac{F_v / F_m}{F_{vM} / F_{mM}}$$

Φ_{PSII}: the photochemical efficiency of functional PSII centres; Φ_{NPQ}: ΔpH dependent, xanthophyll-cycle coupled non-photochemical quenching; $\Phi_{f,D}$: fluorescence/thermal dissipation of the absorbed energy; Φ_{NF}: the thermal dissipation by inactive PSII centers; F_{mM}: the mean of quasi non-inhibited control F_m values. The intensity of actinic light was low enough not to cause additional photoinactivation of PSII centres.

2.5 Thylakoid proteomics

188 Sugar beet leaves from the differently treated plants were used for isolation of thylakoid
189 membranes according to Jansson et al. (1997), with four biological replicates. Thylakoids (0.5
190 mg Chl mL^{-1} in the controls and 0.3 mg Chl mL^{-1} in the Cd-treated and Fe-deficient
191 thylakoids, respectively) were solubilised with 750 mM aminocaproic acid, 50 mM BisTris-
192 HCl (pH 7.0), 0.5 mM EDTA, 250 µg/mL Pefabloc (serine protease inhibitor) and 2% (w/v)
193 n-dodecyl-*β*-D-maltoside on ice for 30 min. After a 15-min centrifugation at 18,000 g at 4 ^{o}C,
194 the supernatant was supplemented with 1/5 volume of 5% (w/v) Serva blue G dissolved in
195 500 mM aminocaproic acid. The use of different Chl concentrations in the controls and the
196 treatments was necessary to optimize the resolution of bands and led to different
197 detergent/Chl ratios. The final Chl load was 10 and 5 µg per lane in the case of controls and
198 the other two treatments, respectively. The protein/Chl ratio was 1.5-2.0 in thylakoids from
199 control and Cd-treated plants and 3.2-4.7 in those from Fe-deficient plants.

200 For separation of the pigment-protein complexes, 1-DE electrophoresis was run under
201 native conditions using BN PAGE (Kügler et al., 1997) in 5-12% (w/v) acrylamide gradient
202 gels (Mini-Protean, BioRad, Hercules, CA, USA). Electrophoresis was carried out at 4^{o}C,
203 with 5 mA per gel and a maximum of 300 V, for approximately 4 h. Separations were
204 repeated four times with each biological replicate. Gels were scanned using an Epson
205 Perfection scanner 4990 in 24-bit colour at 600 dpi, saved in tiff format and images
206 transformed to 8-bit grayscale .tiff files using Photoshop (Adobe Photoshop 12.0.4). To
207 compare the changes occurring in the amount of the different pigment-protein complexes
208 (bands in the 1-DE BN PAGE gels) with the treatments, densitometric analysis (pixel density)
209 was carried out using the Phoretix image analysis software (Phoretix International, UK). The
210 pixel density (that originates from the blue Coomassie and green/yellow photosynthetic
211 pigment colours) is a valid tool to assess the amount of a given pigment-protein complex
212 across treatments, because Coomassie measures quantitatively proteins and neither the protein

composition nor the pigment complement of each complex changed with the treatments (see Results). Since the amounts of thylakoids loaded in each gel were not identical, the total optical density of each lane was normalized using the amount of Chl loaded (1 µg of Chl gave 204585±15216 optical density units).

The apoprotein composition of the different pigment-protein complexes was analyzed in a second dimension using SDS PAGE (Laemmli, 1970). Three mm gel strips cut from a BN PAGE lane were attached to the top of the second dimension denaturing gel (12% w/v) in solubilising buffer containing 0.5% (w/v) agarose, and proteins were separated in the above-mentioned apparatus with a constant current of 20 mA per gel for 2 h. After electrophoresis, gels were stained with colloidal Coomassie blue G-250 (Candiano et al., 2004). Gels were scanned using an Epson Perfection scanner 4990 in 8-bit grayscale at 600 dpi, saved in tiff format and analyzed with the Phoretix image analysis software as indicated above. The optical density values of all the polypeptides present in the 2-DE BN/SDS gels was used to assess the changes in the relative distribution of different protein complexes with the treatments, except in the case of the different PSII forms that were assessed according to the distribution of the CP47 apoproteins.

2.6. Protein in Gel Digestion and Identification by Nanoliquid Chromatography-Tandem Mass Spectrometry (nLC−ESI−MS/MS)

Some polypeptide spots could be unequivocally identified on the basis of earlier results using similar gel systems for separation of polypeptides of PSI (Nelson and Yokum, 2006), PSII (Aro et al., 2005), ATP synthase (Seelert at el., 2003), and Cyt b_6f complex (Suh et al., 2000).

Spots were excised automatically from the Coomassie-stained gels using a spot cutter EXQuest (BioRad), and *in gel*-digested with trypsin as indicated elsewhere (Rodríguez-Celma et al., 2013). Peptide mixtures were analysed with a nano-HPLC system 1200 series (Agilent

Technologies) connected to a HCT Ultra high-capacity ion trap (Bruker Daltoniks, Bremen, Germany) using a PicoTip emitter (50 μm i.d., 8 μm tip i.d., New Objective, Woburn, MA, USA) and an on line nano-electrospray source (Rodríguez-Celma et al., 2013). Protein identification was performed by searching in the non-redundant NCBInr 20110129 (12806714 sequences; 4372843424 residues) and Plants_EST EST_105 (136442070 sequences; 23838005216 residues) databases, using the MASCOT server (Matrix Science, www.matrixscience.com, London, UK). Searches were carried out using a mass window of 50-100 ppm for the precursor with monoisotopic mass accuracy, and fragment mass tolerance was ±0.6 Da. The search parameters allowed for carbamidomethylation (Cys), oxidation of methionine and allowed fixed modification. Positive identification was assigned with MASCOT scores above the threshold level ($p<0.05$) and were validated manually with a score above homology, great sequence coverage and similar experimental and theoretical MW and pI (Supplementary Table 1). We used the GO biological process annotation (http://www.geneontology.org) of the individual identified proteins for classification.

2.7. Statistical analysis

InStat v. 3.00 (GraphPad Software Inc., La Jolla, CA, USA) was used to carry out ANOVA analysis and a Tukey-Kramer post-test (using a $p\leq0.05$ significance level).

3. Results

3.1. Photosynthetic characteristics and mineral content of leaves from control and treated plants

After the 10-d treatment, sugar beet plants showed characteristic symptoms of Cd toxicity and Fe deficiency, including slower growth and leaf chlorosis. Leaf Chl concentration showed a marked decline both under Cd stress and Fe deficiency, with a preferential loss of Chl *b* as indicated by the increases in Chl *a*/Chl *b* ratios (Table 1). Two groups of Fe-deficient plants

were taken into consideration, one showing a moderate decline in Chl concentration (-Fe) and a second extremely Fe deficient group (-Fe^{Ext}), showing more marked leaf Chl decreases. Further studies were mostly focused on the –Fe^{Ext} plants, since their leaf Chl concentration was similar to that of the leaves from Cd-treated plants (Table 1).

Photosystem II efficiencies decreased under Cd toxicity and extreme Fe deficiency (Table 2). Under Cd stress, both the maximal (F_v/F_m) and the actual ($\Delta F/F_m'$) PSII efficiencies were markedly reduced, whereas Fe deficiency affected photochemical efficiency only moderately. However, NPQ was increased markedly by both Cd toxicity and Fe deficiency (1.7- and 1.6-fold, respectively). Concerning the different mechanisms of energy dissipation, the proportions of Φ_{NPQ} (ΔpH dependent, xanthophyll-cycle coupled non-photochemical quenching) and $\Phi_{f,D}$ (fluorescence/thermal dissipation of the absorbed energy) changed only slightly. However, Φ_{NF} (the thermal dissipation by inactive PSII centers) increased, mainly at the expense of Φ_{PSII} (the photochemical efficiency of functional ones), and this was more intense in Cd treated plants.

Leaves of Cd-treated plants accumulated high levels of Cd, whereas leaves of control and Fe-deficient plants showed very low Cd concentrations (Table 3). Regarding macronutrients, the concentrations of Mg decreased in all treatments, whereas those of Ca increased significantly in the +Cd and –Fe^{Ext} treatments and those of K did not change significantly. Regarding micronutrients, leaf Mn concentrations decreased in all treatments, whereas those of Fe decreased significantly in the +Cd and –Fe^{Ext} treatments, and those of Zn did not change significantly.

The Fe content of isolated intact control chloroplasts was 707.0±111.6 amol Fe chloroplast^{-1}, whereas chloroplasts isolated from Cd treated and –Fe^{Ext} plants contained 370.9±54.9 and 292.5±65.8 amol Fe chloroplast^{-1} (corresponding to approximately 43-57% and 32-50% of the control values), respectively.

3.2. Changes in the amount and organization of the thylakoid complexes revealed by 1-DE BN and 2-DE BN-SDS PAGE

The electrophoretic profiles of the pigment-protein complexes (1-DE BN PAGE; Fig. 1A) and their polypeptide composition (2-DE BN-SDS PAGE; Fig. 1B) were similar in thylakoids from the controls and from leaves affected by extreme Fe deficiency. Similar results were obtained with thylakoids from Cd-stressed and moderate Fe deficiency (Supplementary Fig. 1). A total of 13 bands were observed in the first dimension BN PAGE gels, some of them of green colour (bands *1-7* and *10*) and others where the blue Coomassie colour was predominant (*8-9*, and *11-13*). All these bands were identified according to their polypeptide patterns (Fig. 1B).

Among the first 5 bands of low electrophoretic mobility, bands *1*, *2* and *4* were identified as supercomplexes containing PSI, though the polypeptide composition could not be resolved because of their small amount. Bands *3* and *5* contained mega-/supercomplexes of PSII *core* with its connecting antenna (CA) and outer antenna LHCII, probably differing in the amount of LHCII antenna bound to the complex. Band *6* at 580 kDa molecular mass contained the monomer PSI, ATPase and the dimer PSII complex. PSI core complexes devoid of the antennae together with the CF_1 part of ATPase were present as one or more bands appearing around 425 kDa, and this region was labeled as band *7*. Band *8* had an approximate 315 kDa molecular mass and contained PSII *core* monomer and Cyt b_6f dimer. Band *9* contained PSII *core* monomer without one of its inner antenna, CP43 (PsbC), whereas CP43 appeared alone around 109 kDa (band *12*). The intense green band *10* with 155 kDa molecular mass consisted in LHCII trimers. Band number *11* was identified as Cyt b_6f monomer devoid of the Rieske Fe-S protein. Finally, band *13*, with the fastest electrophoretic mobility (around 90 kDa), contained Lhc monomers.

Based on the polypeptide pattern of the second dimension SDS gels, components of PSII could be distinguished well in the supercomplexes (bands *3* and *5*). The LHCII trimer was found at 75 kDa, although in the native gel it had a molecular mass of 155 kDa. This can be explained by the fact that in this system these proteins can bind Chl even in the second dimension SDS-PAGE separation. Below the trimer, CP47 (PsbB) and CP43 (PsbC) apoproteins were found, followed by D2/D1 (PsbD/PsbA) and the apoproteins of the connecting antenna CP29 (Lhcb4) and CP26 (Lhcb5). Polypeptides of PSI particles were found in band *6* and *7*. Regarding band *6*, Chl-binding PsaA/PsaB/Lhca supercomplex had the highest molecular mass, and among proteins of higher mobility, several *core* components (PsaD, PsaF and PsaL) and an Lhca-type apoprotein (22 kDa) were found. ATP synthase components included the double band composed of the α (AtpA) and β (AtpB; spot *4*) subunits of CF_1 in the 55 kDa region, and the γ (AtpC) subunit at 35 kDa (band *6* and *7*). The small ATP-ase subunits found in the 10-20 kDa region of the 2-DE gels, such as AtpD, CF_o-II, and AtpE, were only detected in band *6*.

Polypeptides of the Cyt b_6f complex, Cyt *f* (PetA), Cyt b_6 (PetB) Rieske Fe-S protein (PetC) and subunit IV (PetD), were found in bands *8* and *11* (in the latter band, PetC was not detected). Apoproteins of the LHCII and the Lhc monomers fall between 20-30 kDa in the region of band *12* (spots *10-12*). In the vicinity of the Lhc monomer band, an aggregate was found which contained Lhcb8 (spot *5*). The 33 kDa molecular weight OEE1 protein of the water splitting complex was also seen in the region corresponding to band *13* (spot *9*).

Polypeptide profiles of thylakoids observed in the 2-DE BN SDS gels were similar to the control in those obtained from plants affected by Cd-toxicity or Fe-deficiency (Fig. 1B, Supplementary Fig. 1). The only exception was the appearance of an enzyme complex in thylakoid preparations from Fe-deficient plants that included aldolase and ferredoxin-$NADP^+$ oxidoreductase (FNR) (spots *6, 7* and *8* in Fig. 1B), at approximately 180 kD in 1-DE gels,

335 which was hardly detected in those from control (Fig. 1B) and Cd-treated plants
336 (Supplementary Fig. 1). This complex could not be distinguished as a separate coloured band
337 in the 1-DE gels.

338 Cadmium toxicity and Fe deficiency led to marked changes in the amount of the different
339 pigment-protein complexes (Fig. 2). Changes were assessed using the pixel density of the
340 different bands in the 1-DE BN PAGE gels [in the case of band *6* the contribution of the PSI
341 monomer (*6'*) and the PSII dimer (*6"*) were estimated from the 2-DE gel by comparing the
342 density ratio of the CP47 apoprotein (PsbB) in band *6* with that of band *8*, which contains
343 only PSII monomer]. Cadmium treatment decreased the amounts of PSII mega-
344 /supercomplexes (bands *3* and *5*), PSI (bands *1*, *2*, *4*, *6'* and *7*) and LHCII trimer (band *10*) by
345 approximately 70%, whereas the amounts of PSII dimer (band *6"*), PSII monomer (band *8*)
346 and Lhc monomers (band *13*) were reduced by approximately 50-60%, and that of the CP43-
347 less PSII core (band *9*) was lowered by less than 50%. In moderately Fe-deficient samples,
348 the amounts of PSI, PSII supercomplexes, PSII monomers, and LHCII trimers decreased to
349 similar extents to those in Cd-treated thylakoids, whereas the PSII dimer was less reduced,
350 and the amounts of CP43-less PSII core and Lhc monomers were similar to those in the
351 control. In samples severely Fe-deficient (-Fe^{Ext}) the pattern was quite similar to those of
352 samples from Cd treated plants, with a significantly stronger reduction detected in the case of
353 PSII supercomplexes and LHCII trimer.

354 The same data were analysed to get information about treatments-induced changes in the
355 ratios between the different types of thylakoid complexes (Fig. 3). The PSI/PSII ratio
356 (assessed from the ratio [bands *1*, *2*, *4*, *6'* and *7*]/[bands *3*, *5*, 6", *8* and *9*]) did not change
357 under either Cd stress or Fe deficiency. However, the LHCII trimer/PSII ratio (calculated as
358 the ratio [band *10*]/[bands *3*, *5*, 6", *8* and *9*]) decreased significantly in the Fe-deficient
359 samples, whereas the LHCII trimer/Lhc monomer ratio (calculated as the ratio [band

10]/[band *13*]) was decreased by both Cd toxicity and Fe deficiency, with a stronger effect in the latter case.

The changes in the relative distribution of different PSI and PSII protein complexes in the samples were assessed from the optical density values of the polypeptides present in the 2-DE BN-SDS PAGE gels (Fig. 4A and 4B for PSI and PSII, respectively; see gels in Fig. 1B). In the case of PSII complexes the ratios were calculated on the base of CP47 spots, as this protein is present in each of the complexes and its amount is directly proportional to the complex. In the case of PSI the only significant change was a reduction in PSI monomer (band *6'*) in the case of the extremely Fe-deficient samples; the organization of PSI did not change with Cd treatment. However, marked changes were induced in the organization of PSII by all the treatments (Fig. 4B). In control samples, the PSII monomer (band *8*) was the most abundant (33%), followed by PSII supercomplexes (bands *3* and *5*) and dimers (band *6''*) (23 and 24%, respectively), and the CP43-less PSII core monomer (band *9*) (about 20%). Cadmium treatment decreased significantly the proportion of PSII supercomplexes, while that of CP43-less PSII *core* increased significantly and the proportions of PSII dimer and monomer did not change. Similar organization changes were observed in thylakoids from Fe-deficient plants. In moderately Fe-deficient plants, the proportion of the CP43-less PSII was almost two-fold compared to the control, at the expense of PSII supercomplexes and monomers.

The changes in the relative amount of other complexes and soluble proteins bound to thylakoids were also assessed from the optical density values of all the polypeptides present in the 2-DE BN-SDS PAGE gels (Fig. 5; see gels in Fig. 1B). There was an increasing trend in the amount of ATP synthase (in bands *6* and *7*), which was significant in extremely Fe-deficient thylakoids. Moreover, a significant increase in the CF_1/CF_o+CF_1 ratio was also detected both in the Cd treated and extremely Fe-deficient samples but not in the moderately

Fe-deficient ones. While the total amount of Cyt b_6f complex (in bands *8* and *11*) did not change significantly in the treated samples, the dimer/monomer ratio increased in Cd treated and extremely Fe-deficient ones. The amounts of Rubisco (in band *6* and zone at approximately 500 kD in the 1-DE BN PAGE gels) and that of the complex including aldolase and FNR (zone at approximately 180 kD in the 1-DE BN PAGE gels) increased significantly in extremely Fe-deficient plants when compared to the controls.

3.3. Carotenoid composition of pigment-protein bands separated by 1-DE BN PAGE

The carotenoid composition of the pigment-protein complexes separated from the treated thylakoids was similar to that of the corresponding controls (see Supplementary Fig. 2). Core complexes contained mainly *ß*-carotene), whereas in the antenna complexes lutein, VAZ (violaxanthin-antheraxanthin-zeaxanthin), and neoxanthin were the main carotenoids.

The VAZ/lutein ratio was high in the PSI+PSII dimer (band *6*) and Lhc monomer bands (band *13*), and it was very low in LHCII trimers (band *10*) (Fig. 6). The markedly increased amount of VAZ pigments observed in extremely Fe-deficient leaves (Fig. 6) could not be detected in any of the main bands of the BN gels.

4. Discussion

In plants, the effects of Cd toxicity are generally intertwined to others caused by a Cd-induced Fe deficiency. For instance, it has been reported that a Cd-induced Fe deficiency in leaves is deeply involved in the effects of Cd on photosynthesis (Siedlecka and Krupa, 1999; Larbi et al., 2002), and that during Cd exposure, the loss and Fe-dependent recovery of the thylakoid apparatus and photosynthetic activity are closely related to Fe availability (Sárvári et al., 1999; Shao et al., 2007; Solti et al., 2008). To further investigate the contribution of Fe deficiency to Cd stress symptoms, the composition and organization changes of the thylakoid complexes were compared in plants grown under these two stresses using 1-DE BN and 2-DE

409 BN-SDS PAGE, combined with mass spectrometry along with parallel studies on functional
410 changes. Sugar beet plants were chosen as model plants, as they have been shown to be
411 sensitive both to Cd exposure (Larbi et al., 2002) and Fe deficiency (Larbi et al., 2006).

412 Both Cd toxicity and Fe deficiency caused strong leaf chlorosis in sugar beet, with the final
413 leaf Chl concentrations being similar in leaves of plants grown with Cd and in extremely Fe-
414 deficient condition. These changes in Chl are in full agreement with the changes found in
415 chloroplast Fe contents, which were also similar in Cd-treated and extremely Fe-deficient
416 plants. This, along with the fact that leaf Fe concentrations in plants grown with Cd were
417 significantly higher than that found in extremely Fe-deficient leaves, supports that Cd impairs
418 significantly chloroplast Fe supply in leaves. The decrease in Chl is likely to be associated to
419 the shortage of Fe. Fe deficiency is known to affect several enzymatic steps in Chl
420 biosynthesis, including the functioning and biosynthesis of Mg-protoporfirin-IX-monomethyl-
421 ester oxidative cyclase (Yang et al., 2010) and chlorophyll *a* oxygenase (Tanaka et al., 1998).
422 In addition, Fe is important part of many of the components of the photosynthetic machinery
423 (Terry and Abadía, 1986).

424 The decreases in leaf Chl concentrations and the parallel increases in the Chl *a/b* ratio
425 indicate that the photosynthetic apparatus undergoes a significant reorganization under both
426 Cd toxicity and Fe-deficiency. The major changes found to be concerned the relative amount
427 of multi-protein complexes, whereas the 1-DE BN-PAGE band patterns of thylakoids from
428 control and treated plants did not differ qualitatively, and the polypeptide and carotenoid
429 composition of the corresponding BN bands was also similar.

430 Based on the densitometry analysis of the BN gels, the most sensitive complexes were
431 those containing PSI and LHCII during both Cd treatment and Fe deficiency, in agreement
432 with previous results obtained in Fe-deficient sugar beet and spinach (Andaluz et al., 2006;
433 Timperio et al., 2007), as well as in Cd-treated cucumber, poplar, spinach and Indian mustard

plants (Sárvári et al., 1999; Sárvári, 2005; Fagioni et al., 2009; Qureshi et al., 2010). PSI and LHCII are the most abundant thylakoid complexes (see legend of Fig. 2), and therefore they are strongly influenced by the decrease in leaf Chl. In addition, PSI complexes contain a high amount of Fe in the form of Fe-S centres (12 Fe per PSI unit), which are structurally important for the stabilization of the complexes (Amann et al., 2004). The decrease in the amount of Lhcs can be related not only to the Fe deficiency-induced loss of stabilizing Chls (Hoober et al., 2007), but also to both the influence of Cd on the expression of *Lhc* genes (Tziveleka et al., 1999; Fusco et al., 2005) and the acclimation trend of stressed plants towards a decreased antenna size (Timperio et al., 2007; Laganowsky et al., 2009).

Regarding the organisation of PSI, proportions of the supercomplexes together with the core complexes tended to be increased in Fe-deficient thylakoids, but a significant decrease in monomeric PSI was only detected in extremely Fe-deficient plants. PSI supercomplexes most probably represent NAD(P)H dehydrogenase-PSI (NDH-PSI) supercomplexes participating in cyclic electron flow (Peng et al., 2008). Thus, the higher proportion of PSI supercomplexes may be a sign of a higher contribution of cyclic electron flow to the excess light energy quenching processes. An increase in the proportion of the membrane bound FNR supposed to participate in cyclic electron flow (Benz et al., 2010) was also observed in the case of extremely Fe-deficient thylakoids together with an increased abundance of ATP synthase and a higher stability of the Cyt b_6f dimers. Results found here confirm those of a previous study (Andaluz et al., 2006), namely that some of the chloroplast stromal proteins, such as the Rubisco large subunit, plastid aldolase, and an unknown protein containing a FNR domain were still present in Fe-deficient sugar beet thylakoid preparations even after an extensive washing, with the amount of some ATPase subunits being also high. Supporting the above mentioned hypothesis, Fe deficiency was found to increase the amount of Lhcb1 and Lhcb2 proteins in PSI complexes and stroma lamellae of spinach leaves (Timperio et al., 2007), and

459 to cause post-translational modifications of PsaH2 protein (involved in the binding of Lhcb
460 proteins to PSI) in Arabidopsis (Laganowsky et al., 2009), which may contribute to the light
461 harvesting efficiency of PSI participating in cyclic electron flow. Iron deficiency also induced
462 an increase in cyclic electron flow in cyanobacteria (Michel and Pistorius, 2004). Similar
463 changes were not found in thylakoids of Cd treated plants, suggesting that cyclic electron
464 flow is relevant as a protective mechanism under Fe deficiency but not under Cd stress.

465 The observed PSII organizational changes can be related to the strong Cd-induced Fe
466 deficiency, since they were quite similar in Cd treated and extremely Fe-deficient thylakoids.
467 PSII mega-/supercomplexes differing in the amount of LHCII trimer and/or being in different
468 oligomerization state were the most sensitive to both stresses. This is likely related to the high
469 sensitivity of Lhcb4 and Lhcb6 to Fe deficiency (Timperio et al., 2007), since these
470 connecting antennae are essential for the formation of super- and megacomplexes (Dekker
471 and Boekema, 2005). The amount of CP43-less PSII core, considered as intermediates in the
472 PSII regeneration cycle (Andersson and Aro, 2001), was somewhat less reduced than that of
473 the other PSII forms, which may be related to the slow regeneration of PSII (Geiken et al.,
474 1998). In moderately Fe-deficient thylakoids, however, the abundance of CP43-less PSII core
475 increased compared to that of the other PSII forms. An increase in the amount of a PSII
476 subcomplex suggesting a higher rate of PSII repair was also shown in *Brassica juncea* (Indian
477 mustard), a less sensitive, hyper-accumulator plant, both under Fe deficiency and Cd
478 treatment (Qureshi et al., 2010). Therefore, moderately Fe-deficient plants may have enough
479 energy to repair PSII damage, whereas energy would be hardly available under strong Fe
480 deprivation or Cd stress.

481 The most obvious change in the organization of complexes was the increased Lhc
482 monomer to trimer ratio in the thylakoids from stressed plants, in agreement with previous
483 results obtained with Cd-treated Indian mustard (Qureshi et al., 2010), and Fe-deficient sugar

beet and spinach (Andaluz et al. 2006, Timperio et al. 2007, respectively). It was demonstrated that light energy can be quenched more easily when absorbed by the monomeric Lhc-s than by the trimeric form (Garab et al., 2002). The observed changes can be the consequence of changed Lhcb isoforms, which are known to influence the organization of both PSII supercomplexes (Damkjær et al., 2009) and LHCII (Caffari et al., 2005). In agreement, transcriptome analysis of Fe-deficient barley plants revealed that two of the *Lhcb1* genes had an elevated level of expression with a concomitant increase of monomeric Lhcb1 proteins (Saito et al., 2010). Distinct changes in Lhcbs were found in other species suggesting that acclimation may be species-specific (Andaluz et al. 2006, Timperio et al. 2007, Laganowsky et al. 2009). This question has not been discussed yet in the context of Cd stress. According to our results obtained with poplar, a subpopulation of both *Lhca* and *Lhcb* genes could play a crucial role in acclimation under Cd-exposure (unpublished data). We hypothesize that the organizational changes in the Lhc antennae in sugar beet under both Cd stress and Fe deficiency could result in a reduction of the proportion of absorbed energy reaching the reaction centre, thus limiting the degradation of the photosynthetic components caused by photoinhibitory processes.

Changes in the carotenoid composition may also contribute to the protection of photosynthetic apparatus against excess light, particularly in severely Fe-deficient plants, where high amounts of Z accumulate in leaves (Fig. 6; Morales et al., 1990) and thylakoids (Quílez et al., 1992). In chlorophyll *b* and xanthophyll-biosynthesis mutants, xanthophylls were bound loosely to the complexes or occurred as free pigment (Dall'Osto et al., 2010). The location of the large amount of Z in Fe-deficient thylakoids, however, is unknown so far and should be the focus of further studies.

In conclusion, the very similar reorganization of thylakoid complexes, particularly PSII and LHCII, in both extremely Fe-deficient and Cd-stressed plants, supports the pivotal role of

chloroplast Fe deficiency in triggering the acclimation responses under Cd stress. Although the main quenchers under severe Fe depletion, i.e. increased intensity of cyclic electron flow and accumulation of Z, seems not to take part in the protective mechanisms under Cd stress but rather thermal dissipation by inactive PSII complexes. These differences in PSI response and in protective mechanisms under Cd stress can be attributed to a more pronounced inhibition of PSII activity, which is likely to be related to direct or indirect effects of Cd not other Fe deficiency.

5. Acknowledgements

Supported by grants from ERA Chemistry – OTKA (Project NN-84307) to F. F. and Á. S., and from the Spanish Ministry of Economy and Competitivity (MINECO; project AGL2010-16515, co-financed with FEDER), and the Aragón Government (Group A03) to J.A. Authors thank Elain Gutierrez-Carbonell for the measurement of the protein concentration in the thylakoid samples.

6. References

Alcántara, E., Romera, F.J., Cañete, M., de La Guardia, M.D., 1994. Effects of heavy metals on both induction and function of root Fe(III) reductase in Fe-deficient cucumber (*Cucumis sativus* L.) plants. J. Exp. Bot. 45, 1893-1898.

Amann, K., Lezhneva, L., Wanner, G., Herrmann, R.G., Meurer, J., 2004. Accumulation of Photosystem I, a member of a novel gene family is required for accumulation of [4Fe-4S] cluster–containing chloroplast complexes and antenna proteins. Plant Cell 16, 3084-3097.

Andaluz, S., López-Millán, A-F., de las Rivas, J., Aro, E-M., Abadía, J., Abadía, A., 2006. Proteomic profiles of thylakoid membranes and changes in response to iron deficiency. Photosynth. Res. 89, 141–155.

Andersson, B., Aro, E.M., 2001. Photodamage and D1 protein turnover in Photosystem II. In: Aro, E.M., Andersson, B. (Eds.), Regulation of Photosynthesis Dordrecht/Boston/London, Kluwer Acad. Publ., pp. 377-393.

Aro, E.M., Suorsa, M., Rokka, A., Allahverdiyeva, Y., Paakkarinen, V., Saleem, A., Battchikova, N., Rintamäki, E., 2005. Dynamics of photosystem II: a proteomic approach to thylakoid protein complexes. J. Exp. Bot. 56, 347-356.

Baryla, A., Carrier, P., Frank, F., Coulomb, C., Sahut, C., Havaux, M., 2001. Leaf chlorosis in oilseed rape plants (*Brassica napus*) grown on cadmium-polluted soil: causes and consequences for photosynthesis and growth. Planta 212, 696–709.

Belkhodja, R., Morales, F., Quílez, R., López-Millán, A.F., Abadía, A., Abadía, J., 1998. Iron deficiency causes changes in chlorophyll fluorescence due to the reduction in the dark of the photosystem II acceptor side. Photosynth. Res. 56, 265–276.

Benz, J.P., Lintala, M., Soll, J., Mulo, P., Bölter, B., 2010. A new concept for ferredoxin–NADP(H) oxidoreductase binding to plant thylakoids. Trends Plant Sci. 15, 608-613.

548 Bertrand, M., Poirier, I., 2005. Photosynthetic organisms and excess of metals.
549 Photosynthetica 42, 345-353.

550 Betterle, N., Ballottari, M., Zorzan, S., de Bianchi, S., Cazzaniga, S., Dall'Osto, L.,
551 Morosinotto, T., Bassi, R., 2009. Light-induced dissociation of an antenna hetero-oligomer is
552 needed for non-photochemical quenching induction. J. Biol. Chem. 284, 15255–15266.

553 Caffarri, S., Frigerio, S., Olivieri, E., Righetti, P.G., Bassi, R., 2005. Differential
554 accumulation of *Lhcb* gene products in thylakoid membranes of *Zea mays* plants grown under
555 contrasting light and temperature conditions. Proteomics 5, 758-768.

556 Candiano, G., Bruschi, M., Musante, L., Santucci, L., Ghiggeri, G.M., Carnemolla, B.,
557 Orecchia, P., Zardi, L., Righetti, P.G., 2004. Blue silver: A very sensitive colloidal Coomassie
558 G-250 staining for proteome analysis. Electrophoresis 25, 1327–1333.

559 Chang, Y-Ch., Zouari, M., Gogorcena, Y., Lucena, J.J., Abadía, J., 2003. Effects of cadmium
560 and lead on ferric chelate reductase activities in sugar beet roots. Plant Physiol. Biochem. 41,
561 999-1005.

562 DalCorso, G., Pesaresi, P., Masiero, S., Aseeva, E., Schünemann, D., Finazzi, G., Joliot, P.,
563 Barbato, R., Leister, D., 2008. A complex containing PGRL1 and PGR5 is involved in the
564 switch between linear and cyclic electron flow in Arabidopsis. Cell 132, 273–285.

565 Dall'Osto, L., Cazzaniga, S., Havaux, M., Bassi, R., 2010. Enhanced photoprotection by
566 protein-bound *vs.* free xanthophyll pools: a comparative analysis of chlorophyll *b* and
567 xanthophyll biosynthesis mutants. Mol. Plant. 3, 576–593.

568 Damkjær, J.T., Kereïche, S., Johnson, M.P., Kovács, L., Kiss, A.Z., Boekema, E.J., Ruban,
569 A.V., Horton, P., Jansson, S., 2009. The Photosystem II light-harvesting protein Lhcb3 affects
570 the macrostructure of Photosystem II and the rate of state transitions in Arabidopsis. Plant
571 Cell 21, 3245–3256.

572 Dekker, J.P., Boekema, E.J., 2005. Supramolecular organization of thylakoid membrane
573 proteins in green plants. Biochim. Biophys. Acta 1706, 12–39.

574 Durand, T.C., Sergeant, K., Planchon, S., Carpin, S., Label, P., Morabito, D., Hausman, J-F.,
575 Renaut, J., 2010. Acute metal stress in *Populus tremula* x *P. alba* (717-1B4 genotype): Leaf
576 and cambial proteome changes induced by Cd^{2+}. Proteomics 10, 349–368.

577 Fagioni, M., D'Amici, G.M., Timperio, A.M., Zolla, L., 2009. Proteomic analysis of
578 multiprotein complexes in the thylakoid membrane upon cadmium treatment. J. Proteom. Res.
579 8, 310–326.

580 Faller, P., Kienzler, K., Krieger-Liszkay, A., 2005. Mechanism of Cd^{2+} toxicity: Cd^{2+} inhibits
581 photoactivation of photosystem II by competitive binding to the essential Ca^{2+} site. Biochim.
582 Biophys. Acta 1706, 158-164.

583 Farinati, S., DalCorso, G., Bona, E., Corbella, M., Lampis, S., Cecconi, D., Polati, R., Berta,
584 G., Vallini, G., Furini, A., 2009. Proteomic analysis of *Arabidopsis halleri* shoots in response
585 to the heavy metals cadmium and zinc and rhizosphere microorganisms. Proteomics 9, 4837–
586 4850.

587 Fusco, L.N., Micheletto, L., Corso, G.D., Borgato, L., Furini, A., 2005. Identification of
588 cadmium-regulated genes by cDNA-AFLP in the heavy metal accumulator *Brassica juncea*.
589 J. Exp. Bot. 56, 3017–3027.

590 Fodor, F., Gáspár, L., Morales, F., Gogorcena, Y., Lucena, J.J., Cseh, E., Kröpfl, K., Abadía,
591 J., Sárvári, É., 2005. The effect of two different iron sources on iron and cadmium allocation
592 in cadmium exposed poplar plants (*Populus alba* L.). Tree Physiol. 25, 1173-1180.

593 Garab, G., Cseh, Z., Kovács, L., Rajagopal, S., Várkonyi, Z., Wentworth, M., Mustárdy, L.,
594 Dér, A., Ruban, A.V., Papp, E., Holzenburg, A., Horton, P., 2002. Light-induced trimer to

595 monomer transition in the main light-harvesting antenna complex of plants: thermo-optic
596 mechanism. Biochemistry 41, 15121–15129.

597 Geiken, B., Masojídek, J., Rizzuto, M., Pompili, M.L., Giardi, M.T., 1998. Icorporation of
598 [^{35}S] methionine in higher plants reveals that stimulation of the D1 reaction centre II protein
599 turnover accompanies tolerance to heavy metal stress. Plant Cell Environ. 21, 1265-1273.

600 Hendrickson, L., Förster, B., Pogson, B.J., Chow, W.S., 2005. A simple chlorophyll
601 fluorescence parameter that correlates with the rate coefficient of photoinactivation of
602 Photosystem II. Photosynth. Res. 84, 43–49.

603 Hoober, J.K., Eggink, L.L., Chen, M., 2007. Chlorophylls, ligands and assembly of light-
604 harvesting complexes in chloroplasts. Photosynth. Res. 94, 387–400.

605 Jansson, S., Stefánsson, H., Nyström, U., Gustafsson, P., Albertsson, P-Å., 1997. Antenna
606 protein composition of PSI and PSII in thylakoid sub-domains. Biochim. Biophys. Acta 1320,
607 297-309.

608 Kieffer, P., Schröder, P., Dommes, J., Hoffmann, L., Renaut, J., Hausman, J-F., 2009.
609 Proteomic and enzymatic response of poplar to cadmium stress. J. Proteomics 72, 379–396.

610 Kučera, T., Horáková, H., Šonská, A., 2008. Toxic metal ions in photoautotrophic organisms.
611 Photosynthetica 46, 481-489.

612 Krupa, Z., 1988. Cadmium-induced changes in the composition and structure of the light-
613 harvesting complex II in radish cotyledons. Physiol. Plant. 73, 518-524.

614 Kügler, M., Jänsch, L., Kruft, V., Schmitz, U.K., Braun, H.P., 1997. Analysis of the
615 chloroplast protein complexes by blue-native polyacrylamide gel electrophoresis (BN-
616 PAGE). Photosynth. Res. 53, 35–44.

Laemmli, U.K., 1970. Cleavage of structural proteins during assembly of the head of bacteriophage T4. Nature 227, 680-685.

Laganowsky, A., Gómez, S.M., Whitelegge, J.P., Nishio, J.N., 2009. Hydroponics on a chip: analysis of the Fe deficient Arabidopsis thylakoid membrane proteome. J. Proteomics 72, 397-415.

Larbi, A., Morales, F., Abadía, A., Gogorcena, Y., Lucena, J.J., Abadía, J., 2002. Effects of Cd and Pb in sugar beet plants grown in nutrient solution: induced Fe deficiency and growth inhibition. Funct. Plant Biol. 29, 1453-1464.

Larbi, A., Abadía, A., Morales, F., Abadía, J., 2004. Fe resupply to Fe-deficient sugar beet (*Beta vulgaris L.*) plants induces in the short-term major changes in photosynthetic rate, photosystem II photochemistry and epoxidation state of violaxanthin cycle pigments without significant *de novo* leaf chlorophyll synthesis. Photosynth. Res. 79, 59-69.

Larbi, A., Abadía, A., Abadía, J., Morales, F., 2006. Down co-regulation of light absorption, photochemistry, and carboxylation in Fe-deficient plants growing in different environments. Photosynth. Res. 89, 113–126.

Li, X.P., Muller-Moule, P., Gilmore, A.M., Niyogi, K.K., 2002. PsbS-dependent enhancement of feedback de-excitation protects photosystem II from photoinhibition. Proc. Natl. Acad. Sci. USA 99, 15222–15227.

López-Millán, A-F., Sagardoy, R., Solanas, M., Abadía, A., Abadía, J., 2009. Cadmium toxicity in tomato (*Lycopersicon esculentum*) plants grown in hydroponics. Environ. Exp. Bot. 65, 376-385.

Marschner, H., 1995. Mineral nutrition of higher plants. Academic Press, London.

Michel, K.P., Pistorius, E.K., 2004. Adaptation of the photosynthetic electron transport chain in cyanobacteria to iron deficiency: the function of IdiA and IsiA. Physiol. Plant. 120, 36–50.

641 Miloslavina, Y., Wehner, A., Lambrev, P.H., Wientjes, E., Reus, M., Garab, G., Croce, R.,
642 Holzwarth, A.R., 2008. Far-red fluorescence: a direct spectroscopic marker for LHCII
643 oligomer formation in non-photochemical quenching. FEBS Lett. 582, 3625–3631.

644 Morales, F., Abadía, A., Abadía, J., 1990. Characterization of the xanthophyll cycle and other
645 photosynthetic pigment changes induced by iron deficiency in sugar beet (*Beta vulgaris* L.).
646 Plant Physiol. 94, 607–613.

647 Morales, F., Moise, N., Quilez, R., Abadía, A., Abadía, J., Moya, I., 2001. Iron deficiency
648 interrupts energy transfer from a disconnected part of the antenna to the rest of photosystem
649 II. Photosynth. Res. 70, 207–220.

650 Moseley, J.L., Allinger, T., Herzog, S., Hoerth, P., Wehinger, E., Merchant, S., Hippler, M.,
651 2002. Adaptation to Fe-deficiency requires remodeling of the photosynthetic apparatus.
652 EMBO J. 21, 6709–6720.

653 Nagajyoti, P.C., Lee, K.D., Sreekanth, T.V.M., 2010. Heavy metals, occurrence and toxicity
654 for plants: a review. Environ. Chem. Lett. 8, 199–216.

655 Nelson, N., Yocum, C.F., 2006. Structure and function of photosystem I and II. Ann. Rev.
656 Plant Biol. 57, 521-565.

657 Nilkens, M., Kress, E., Lambrev, P., Miloslavina, Y., Muller, M., Holzwarth, A.R., Jahns, P.,
658 2010. Identification of a slowly inducible zeaxanthin-dependent component of non-
659 photochemical quenching of chlorophyll fluorescence generated under steady-state conditions
660 in *Arabidopsis*. Biochim. Biophys. Acta 1797, 466–475.

661 Padmaja, K., Prasad, D.D.K., Prasad, A.R.K., 1990. Inhibition of chlorophyll synthesis in
662 *Phaseolus vulgaris* L. seedlings by cadmium acetate. Photosynthetica 24, 399-405.

663 Pagliano, C., Raviolo, M., Vecchia F.D., Gabbrielli, R., Gonnelli, C., Rascio, N., et al., 2006.
664 Evidence for PSII donor-side damage and photoinhibition induced by cadmium treatment on
665 rice (*Oryza sativa* L.). J. Photochem. Photobiol. B. Biol. 84, 70–78.

666 Peng, L., Shimizu, H., Shikanai, T., 2008. The chloroplast NAD(P)H dehydrogenase complex
667 interacts with photosystem I in Arabidopsis. J. Biol. Chem. 283, 34873–34879.

668 Porra, R.J., Thompson, W.A., Kriedemann, P.E., 1989. Determination of accurate extinction
669 coefficients and simultaneous equations for assaying chlorophyll a and b extracted with four
670 different solvents: verification of the concentration of chlorophyll standards by atomic
671 absorption spectroscopy. Biochim. Biophys. Acta 975, 384-394.

672 Prasad, M.N.V., 1995. Cadmium toxicity and tolerance in vascular plants. Env. Exp. Bot. 35,
673 525–545.

674 Quílez, R., Abadía, A., Abadía, J., 1992. Characteristics of thylakoids and photosystem II
675 membrane preparations from iron deficient and iron sufficient sugarbeet (*Beta vulgaris* L.). J.
676 Plant Nutr. 15, 1809-1819.

677 Qureshi, M.I., D'Amici, G.M., Fagioni, M., Rinalducci, S., Zolla, L., 2010. Iron stabilizes
678 thylakoid protein-pigment complexes in Indian mustard during Cd-phytoremediation as
679 revealed by BN-SDS-PAGE and ESI-MS/MS. J. Plant Physiol. 167, 761-770.

680 Rodríguez-Celma, J., Lattanzio, G., Jiménez, S., Briat, J.F., Abadía, J., Abadía, A.,
681 Gogorcena, Y., López-Millán, A.F., 2013. Changes induced by Fe deficiency and Fe resupply
682 in the root protein profile of a peach-almond hybrid rootstock. J. Proteom. Res. 12, 1162-
683 1172.

684 Saito, A., Iino, T., Sonoike, K., Miwa, E., Higuchi, K., 2010. Remodelling of the major light-
685 harvesting antenna protein of PSII protects the young leaves of barley (*Hordeum vulgare* L.)
686 from photoinhibition under prolonged iron deficiency. Plant Cell Physiol. 51, 2013–2030.

687 Sanita di Toppi, L., Gabrielli, R., 1999. Response to cadmium in higher plants. Environ. Exp.
688 Bot. 41, 105-130.

689 Sárvári, É., Fodor, F., Csen, E., Varga, A., Záray, G., Zolla, L., 1999. Relationship between
690 changes in ion content of leaves and chlorophyll-protein composition in cucumber under Cd
691 and Pb stress. Z. Naturforsch. 54c, 746-753.

692 Sárvári, É., 2005. Effects of heavy metals on chlorophyll-protein complexes in higher plants:
693 Causes and consequences. In: Handbook of Photosynthesis (M. Pessarakli, ed.), CRC Press,
694 Boca Raton, pp. 865-888.

695 Seelert, H., Dencher, N.A., Müller, D.J., 2003. Fourteen protomers compose the oligomer III
696 of the proton-rotor in spinach chloroplast ATP synthase. J. Mol. Biol. 333, 337-344.

697 Shao, G., Chen, M., Wang, W., Mou, R., Zhang, G., 2007. Iron nutrition affects cadmium
698 accumulation and toxicity in rice plants. Plant Growth Reg. 53, 33-42.

699 Siedlecka, A., Krupa, Z., 1999. Cd/Fe interaction in higher plants – its consequences for the
700 photosynthetic apparatus. Photosynthetica 36, 321-331.

701 Sigfridsson, K.G.V., Bernát, G., Mamedov, F., Styring, S., 2004. Molecular interference of
702 Cd^{2+} with photosystem II. Biochim. Biophys. Acta 1659, 19–31.

703 Solti, Á., Gáspár, L., Mészáros, I., Szigeti, Z., Lévai, L., Sárvári, É., 2008. Impact of iron
704 supply on the kinetics of recovery of photosynthesis in Cd-stressed poplar [*Populus glauca*].
705 Ann. Bot. 102, 771-782.

706 Solti, Á., Kovács, K., Basa, B., Vértes, A., Sárvári, É., Fodor, F., 2012. Uptake and
707 incorporation of iron in sugar beet chloroplasts. Plant Physiol. Biochem. 52, 91-97.

708 Spiller, S.C., Castelfranco, A.M., Castelfranco, P.A., 1982. Effects of iron and oxygen on
709 chlorophyll biosynthesis. I. In vivo observations on iron and oxygen-deficient plants. Plant
710 Physiol. 69, 107-111.

711 Stobart, A.K., Griffiths, W.T., Ameen-Bukhari, I., Sherwood, R.P., 1985. The effect of Cd^{+2}
712 on the biosynthesis of chlorophyll in leaves of barley. Physiol. Plant. 63, 293-298.

713 Suh, H.J., Kim, C.S., Jung, J., 2000. Cytochrome b_6/f complex as an indigenous
714 photodynamic generator of singlet oxygen in thylakoid membranes. Photochem. Photobiol.
715 71, 103-109.

716 Tanaka, A., Ito, H., Tanaka, R., Tanaka, N.K., Yoshida, K., Okada, K., 1998. Chlorophyll *a*
717 oxygenase (*CAO*) is involved in chlorophyll *b* formation from chlorophyll *a*. Proc. Natl.
718 Acad. Sci. USA 95, 12719–12723.

719 Terry, N., Abadía, J., 1986. Function of iron in chloroplasts. J. Plant Nutr. 9, 609-646.

720 Timperio, A.M., D'Amici, G.M., Barta, C., Loreto, F., Zolla, L., 2007. Proteomics, pigment
721 composition, and organization of thylakoid membranes in iron-deficient spinach leaves. J.
722 Exp. Bot. 58, 3695-3710.

723 Tziveleka, L., Kaldis, A., Hegedűs, A., Kissimon, J., Prombona, A., Horváth, G., Argyroudi-
724 Akoyunoglou, J., 1999. The effects of Cd on chlorophyll and light-harvesting complex II
725 biosynthesis in greening plants. Z. Naturforsch. 54c: 740-745.

726 van Assche, F., Clijsters, H., 1990. Effects of metals on enzyme activity in plants. Plant Cell
727 Environ. 13, 195-206.

728 Wilson, K.E., Ivanov, A.G., Öquist, G., Grodzinski, B., Sarhan, F., Huner, N.P.A., 2006.
729 Energy balance, organellar redox status, and acclimation to environmental stress. Canad. J.
730 Bot. 84, 1355-1370.

731 Yang, T.J.W., Lin, W-D., Schmidt, W., 2010. Transcriptional profiling of the *Arabidopsis*
732 iron deficiency response reveals conserved transition metal homeostasis networks. Plant
733 Physiol. 152, 2130–2141.
734

7. Tables

Table 1. Leaf chlorophyll (Chl) concentration and Chl *a* to Chl *b* ratio in control leaves and leaves affected by Cd toxicity and moderate and extreme Fe deficiency. +Cd: Cd treated, –Fe: moderately Fe deficient, -Fe^{Ext}: extremely Fe deficient. * values differing significantly from the controls ($P < 0.05$).

	Control	**+Cd**	**-Fe**	**-Fe^{Ext}**
Chl (µg cm^{-2})	53.1±3.9	19.7±7.6*	25.7±1.9*	16.9±4.3*
Chl *a/b ratio*	3.3±0.1	3.9±0.2*	3.8±0.1*	*5.2±1.5**

Table 2. Photochemical efficiency and energy dissipation parameters in control leaves and leaves affected by Cd toxicity and extreme Fe deficiency (Fe^{Ext}; see Table 1 for treatments). Upper part: parameters for treated leaves are given in the shaded area (in italics) as percentages of those found in the controls. Lower part: proportions (in %) of the different mechanisms of energy dissipation. *values differing significantly from the controls (P <0.05).

	Control	**+Cd**	**-Fe^{Ext}**
F_v/F_m	0.84±*0.01*	*60.2±3.8**	*91.2±6.1**
$\Delta F/F_m'$	0.76±*0.02*	*66.7±3.8**	*87.1±6.1**
NPQ	0.22±*0.08*	*172.8±2.8**	*156.1±10.5**
Φ_{PSII}	73.7±*4.0*	30.4±*2.5**	55.9±*3.7**
Φ_{NF}	2.0±*1.0*	39.8±*0.2**	8.8±*0.6**
Φ_{NPQ}	2.6±*0.8*	8.3±*0.1**	2.6±*0.2*
$\Phi_{f,D}$	21.7±*1.5*	21.5±*1.3*	32.6±*2.2**

Table 3. Mineral composition of control leaves and leaves affected by Cd toxicity and Fe deficiency (see Table 1 for treatments). Cadmium concentrations in all samples and the rest of nutrient concentrations in the control are expressed in μg g^{-1} dry weight. Other nutrient concentrations in the treated leaves are given in the shaded area (in italics) as percentages of the values found in the controls. *values differing significantly from those of the controls ($P < 0.05$).

	Control	**+Cd**	**-Fe**	**-Fe^{Ext}**
Cd	0.9±0.2	633.0±82.3	1.2±0.2	1.2±0.3
K	36774±8337	*108.6±13.7*	*80.8±18.3*	*90.6±4.5*
Ca	18643±492	*144.8±4.0**	*124.3±7.6*	*148.7±3.9**
Mg	17556±6842	*54.3±1.1**	*53.1±20.7**	*37.7±14.7**
Fe	76.0±4.0	*56.1±3.0**	*89.4±4.7*	*24.9±2.7**
Mn	349.3±58.7	*34.2±11.6**	*50.4±8.5**	*15.7±2.6**
Zn	47.1±7.8	*88.5±8.9*	*118.4±19.5*	*127.1±21.0*

758

Supplementary Table 1. Proteins identified in 2-DE BN-SDS PAGE gels. Positive identification was assigned with Mascot scores above the threshold level (P <0.05), at least 2 identified peptides (ion) with a score above homology and 10% sequence coverage. Protein score is –10*Log (P), where P is the probability that the observed match is a random event. Function was inferred from GO:P (biological process-P) annotation.

Spot number	Protein identification	Mass window (ppm)	MASCOT Score	Accesion No. NCBI/ EST	Mascot matches	No. of peptides	Sequence coverage (%)
	PSI core complex						
1	PsaB	100	156	gi|752032	4	2	3
	PsaA	100	82	gi|22091526	2	2	2
	PSI type III chlorophyll a/b-binding [Arabidopsis t.], Lhca3	100	163	gi|430947	3	2	10
3	PS I P700 chlorophyll a apoprotein A2, PsaB [Spinacia oleracea]	100	106	gi|11497524	2	2	3
15	Photosystem I reaction center subunit II, PsaD	75	390	gi|417544	34	6	28
17	Photosystem I reaction center subunit III, PsaF	100	130	gi|131187/ EG551670	3	3	10,5
19	Photosystem I subunit XI precursor , PsaL [Arabidopsis	75	65	gi|5738542	1	1	6

	thaliana]						
	Lhc proteins						
5	LHCB4.3 (light harvesting complex PSII), LHCB8 [Arabidopsis thaliana]	75	124	gi|15225630/BQ489041	2	2	21
10	Type I (26 kD) CP29 polypeptide [Solanum lycopersicum]	75	520	gi|19184/BQ487648	10	7	42
11	LHCB5; chlorophyll binding, CP26 [Arabidopsis thaliana]	75	104	gi|15235028	2	2	9
12	LHCII type I CAB-40, LHCB1 (Nicotiana tabacum)	50	74	gi|19829	2	2	26
13	LHCII type I CAB-36, LHCB1 [Nicotiana tabacum]	75	84	gi|19827	2	1	8
14	PSI type III chlorophyll a/b-binding protein, LHCA3 [Arabidopsis thaliana]	75	155	gi|430947	5	3	14
	ATP synthase						
4	ATP synthase beta subunit [Anagallis arvensis]	75	260	gi|12004131	4	4	15
16	ATP synthase delta chain, chloroplast	100	369	gi|114584/BQ487814	8	4	20

18	ATP synthase beta chain, chloroplast precursor (Subunit II)	100	64	gi|461595	1	1	4
	Membrane associated enzimes						
2	Rubisco Large Subunit	100	143	gi|118624224	4	3	9
9	33 kDa precursor protein of the OEC [Salicornia europaea]	75	363	gi|197691939	17	5	21
20	Thylakoid membrane phosphoprotein 14 kDa, chloroplast precursor, putative [Ricinus communis]	100	59	gi|255541776/ FG345112	2	1	4,6
6	fructose-bisphosphate aldolase, putative [Ricinus communis]	75	240	gi|255581400	17	5	16
7	Ferredoxin--NADP reductase, leaf isozyme, chloroplastic	75	300	gi|119905	9	5	15
8	fructose-bisphosphate aldolase, putative [Ricinus communis]	75	278	gi|255581400	44	6	19

8. Figure captions

Fig 1. (A) 1-DE BN PAGE profiles of thylakoids isolated from leaves of control (Ctrl) and differently treated plants (see Table 1 for treatments). The molecular mass of the complexes was estimated (red numbers on the left) using data published by Fagioni et al. (*2009*) as standards (black numbers). Rubisco – ribulose 1,5-bisphosphate carboxylase-oxigenase. **(B)** 2-DE BN-SDS PAGE polypeptide patterns of thylakoids isolated from leaves of control and extremely iron deficient (-Fe^{Ext}) plants. Polypeptides identified on the basis of previous studies using similar gel systems are marked in black, whereas proteins identified in the present study by nano-HPLC combined with mass spectrometry are marked in red (Supplementary Table 1). FNR – ferredoxin-$NADP^+$ reductase.

Fig. 2. Changes in the amounts of different pigment-protein complexes in 1-DE BN PAGE gels of thylakoids isolated from leaves of plants affected by Cd toxicity and Fe deficiency (see Table 1 for treatments). Changes were estimated from the optical density of the bands and given as percentage of the control value. +Cd: dark grey; -Fe, light grey; -Fe^{Ext}, white. Sum PSI: bands *1*, *2*, *4*, *6*' and *7*; PSII super-complex: bands *3* and *5*; PSII dimer: band *6*"; PSII monomer: band *8*; CP43-less PSII core: band *9*; LHCII trimer: band *10*; Lhc monomers: band *13*. The optical density values for the controls (Fig. 1A) were as follows: Sum PSI, 539927±37245; PSII super-complex, 154748±16135; PSII dimer, 159367±34979; PSII monomer, 217804±38004; CP43-less PSII core, 131751±26066; LHCII trimer, 595840±9229; Lhc monomers, 146385±14154. In the case of band *6*, the contribution of the PSI monomer (*6'*) and the PSII dimer (*6"*) were estimated in the second dimension gel by comparing the density ratio of the CP47 apoprotein (PsbB) in band *6* with that of band *8*, which contains

only PSII monomer. All the values differed significantly from the controls ($P < 0.05$) except the one signed: *****.

Fig. 3. Ratio of pigment-protein complexes estimated from the 1-DE BN PAGE gels of thylakoids from leaves of control plants and plants affected by Cd toxicity and Fe deficiency (see Table 1 for treatments). Control, black; +Cd, dark grey; -Fe, light grey; -Fe^{Ext}, white. LHCII-t – LHCII trimer, Lhc-m – Lhc monomer. The PSI/PSII, LHCII trimer/PSII and LHCII trimer/Lhc monomer ratios were estimated from the optical density of the bands as [bands *1*, *2*, *4*, *6'* and *7*]/[bands *3*, *5*, 6", *8* and *9*]), [band *10*]/[bands *3*, *5*, 6", *8* and *9*]) and [band *10*]/[band *13*]), respectively. *****values differing significantly from the controls ($P < 0.05$).

Fig. 4. Relative distribution of different PSI (A) and PSII (B) protein complexes in thylakoids from leaves of control plants and plants affected by Cd toxicity and Fe deficiency (see Table 1 for treatments), assessed from the 2-DE BN-SDS PAGE gels. The optical density values of all spots present in the second dimension of the different BN bands were used in the assessment, as follows: A) PSI supercomplex, white (bands *1*, *2* and *4*); PSI monomer, light grey (band *6'*); PSI core, dark grey (band *7*). B) PSII mega-/super-complexes, white (bands *3* and *5*); PSII dimer, light grey (band *6*"); PSII monomer, dark grey (band *8*); CP43-less PSII, black (band *9*). In the case of band *6* the contribution of the PSI monomer (*6'*) and the PSII dimer (*6"*) were estimated in the second dimension gel by comparing the density ratio of the CP47 apoprotein (PsbB) in band *6* with that of band *8*, which contains only PSII monomer. *values differing significantly from the control value ($P < 0.05$).

Fig. 5. Changes in the relative amount of other complexes and soluble proteins in thylakoids from leaves of control plants and plants affected by Cd toxicity and Fe deficiency (see Table 1

for treatments), assessed from the 2-DE BN-SDS PAGE gels. The optical density values of the corresponding spots were used to estimate the amounts of ATP synthase (bands *6* and *7*), Cyt b_6f complex (bands *8* and *11*), Rubisco (band *6* and zone at approximately 500 kD in the 1-DE BN gels) and a complex composed of aldolase and FNR (zone at approximately 180 kD in the 1-DE BN gels). Control (black), +Cd (dark grey), -Fe (light grey) and -Fe^{Ext} (white). *values differing significantly from the controls ($P < 0.05$).

Fig. 6. VAZ/lutein ratio in leaves and different 1-DE BN PAGE bands of thylakoids from leaves of control plants and plants affected by Cd toxicity and Fe deficiency. Control (black), +Cd (dark grey), -Fe^{Ext} (white). PSI-m: PSI monomer, PSII-d – PSII dimer, VAZ: violaxanthin-antheraxanthin-zeaxanthin. *****value differing significantly from the controls ($P < 0.05$).

Supplementary Fig. 1. 1-DE (upper horizontal gel bands) and 2-DE BN-SDS PAGE polypeptide patterns of thylakoids isolated from leaves of Cd-treated (**A**) and moderately Fe deficient (**B**) plants. Numbered lanes are: 1,2,4: PSI supercomplexes; 1,3,5: PSII supercomplexes; 6: PSI (RCI+LHCI), PSII *core* dimer, ATPase, Rubisco; 7: PSI *core*, ATPase CF1; 8: PSII *core* monomer, Cyt b_6f dimer; 9: CP43-less PSII core; 10: LHCII trimer; 11: Cyt b_6f monomer; 12: CP43; 13: Lhc monomer. Some of the characteristic polypeptides identified on the basis of previous studies using similar gel systems are marked (See Fig.1).

Supplementary Fig. 2. Carotenoid composition of BN bands belonging to thylakoids isolated from leaves of control plants and plants affected by Cd toxicity and Fe deficiency (see Table 1 for treatments). Control (black), +Cd (dark grey), -Fe^{Ext} (white). VAZ: violaxantin-antheraxanthin-zeaxanthin. A: PSII mega/supercomplexes (bands *3,5*), B: PSI monomer and

PSII dimer (band *6*), C: PSII *core* monomer (band *8*) D: CP43-less PSII *core* (band *9*), E: LHCII trimer (band *10*), F: Lhc monomers (band *13*).

9. Figures

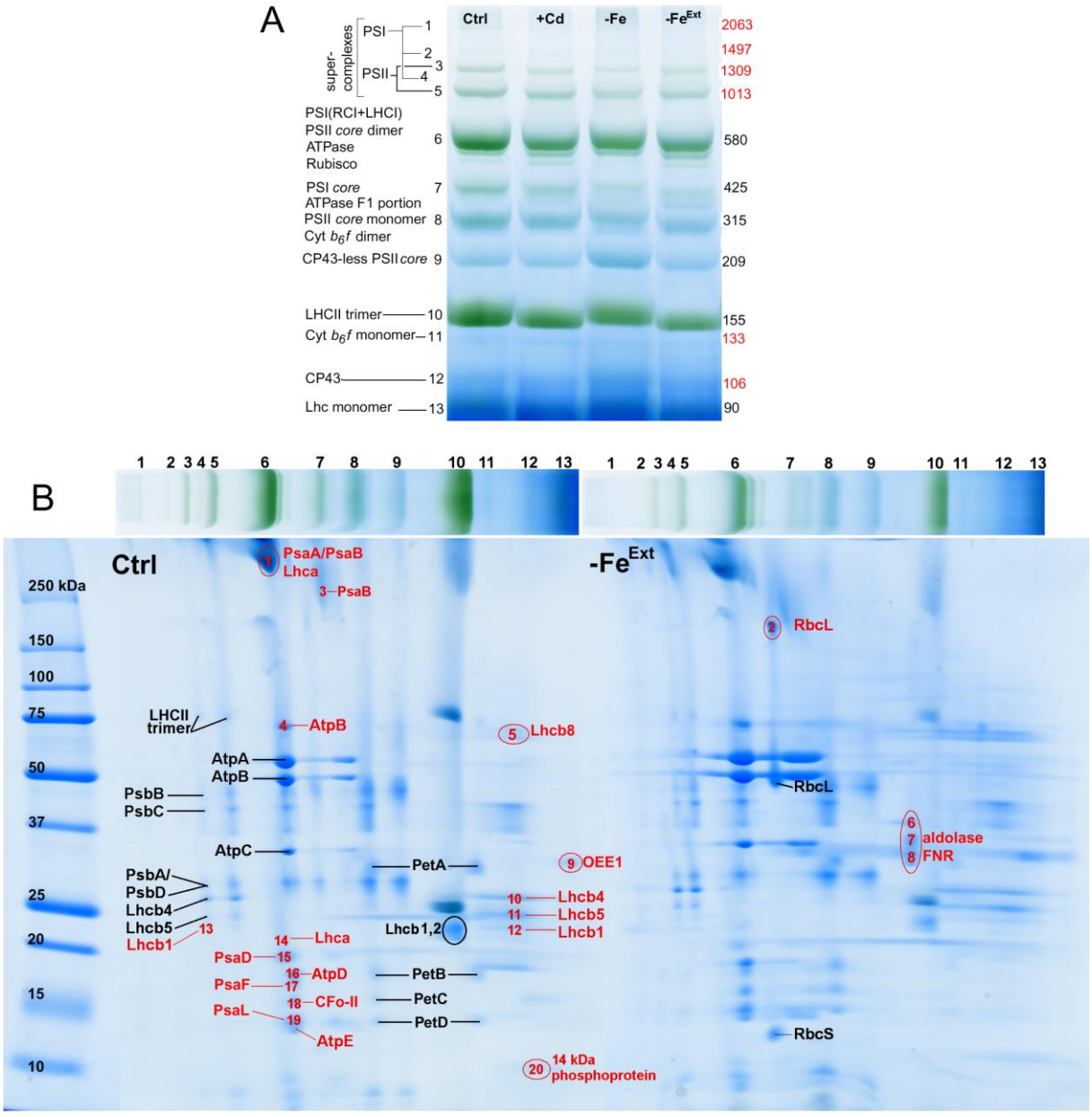

Figure 1.

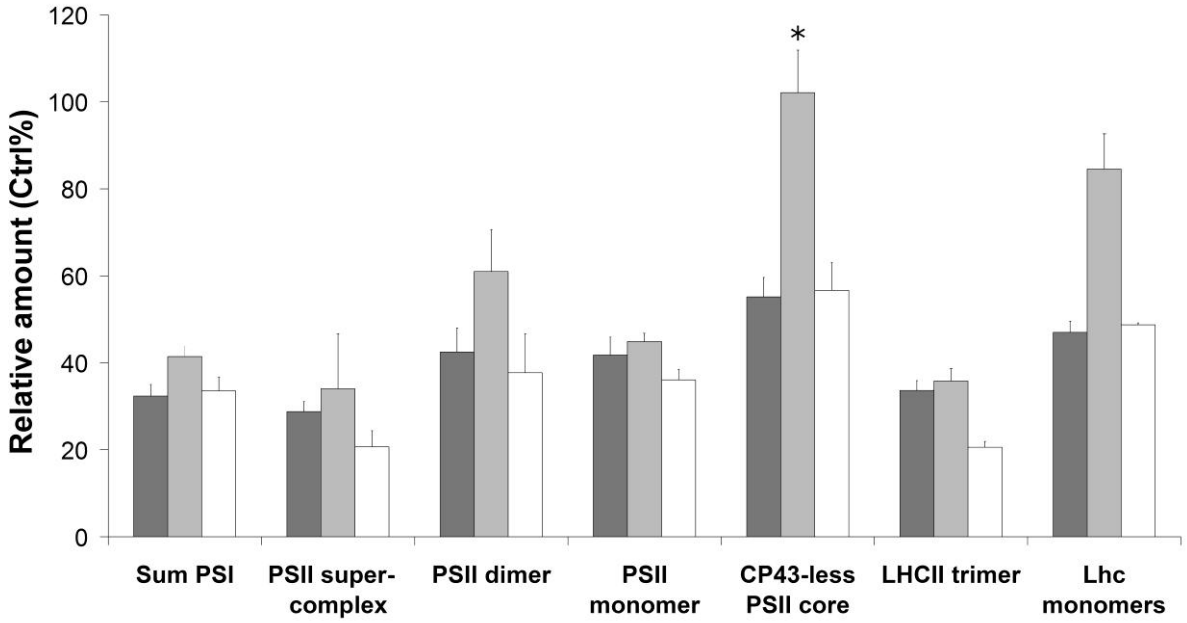
120
100
80
60
40
20
0
Relative amount (Ctrl%)
*
Sum PSI
PSII super-complex
PSII dimer
PSII monomer
CP43-less PSII core
LHCII trimer
Lhc monomers

Figure 2.

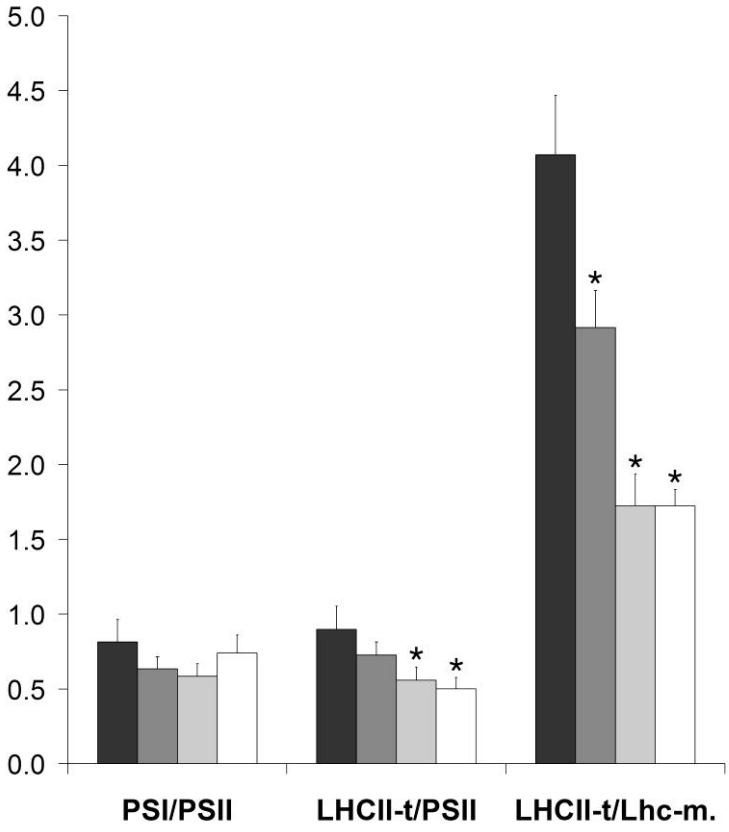

Figure 3.

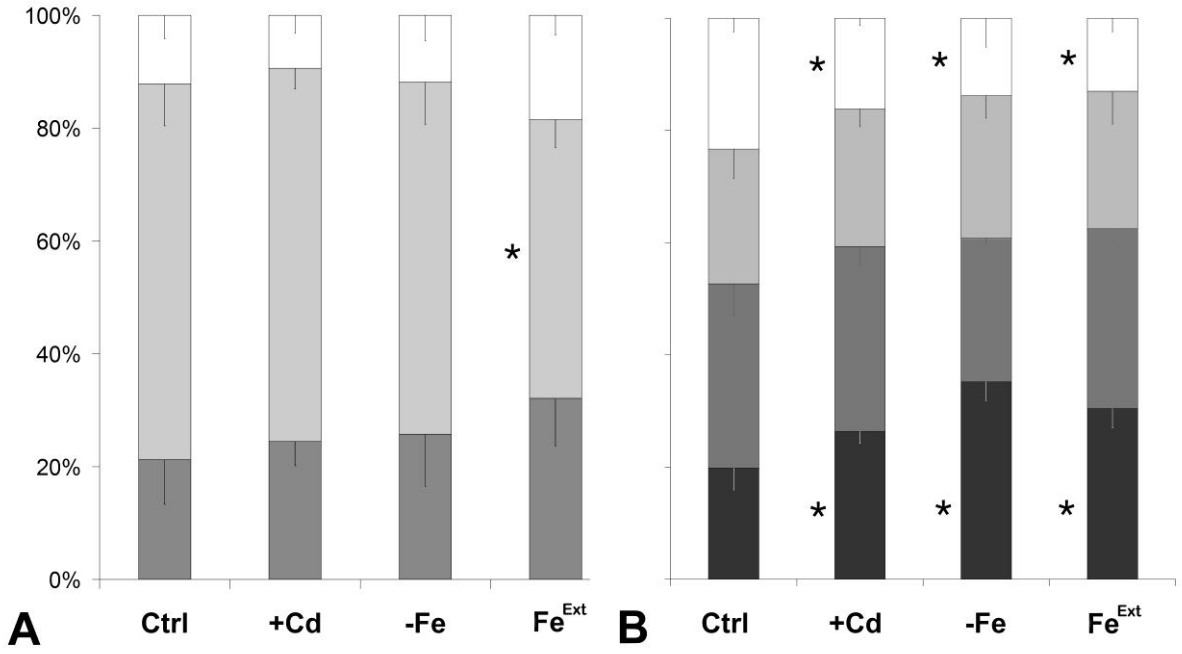

Figure 4.

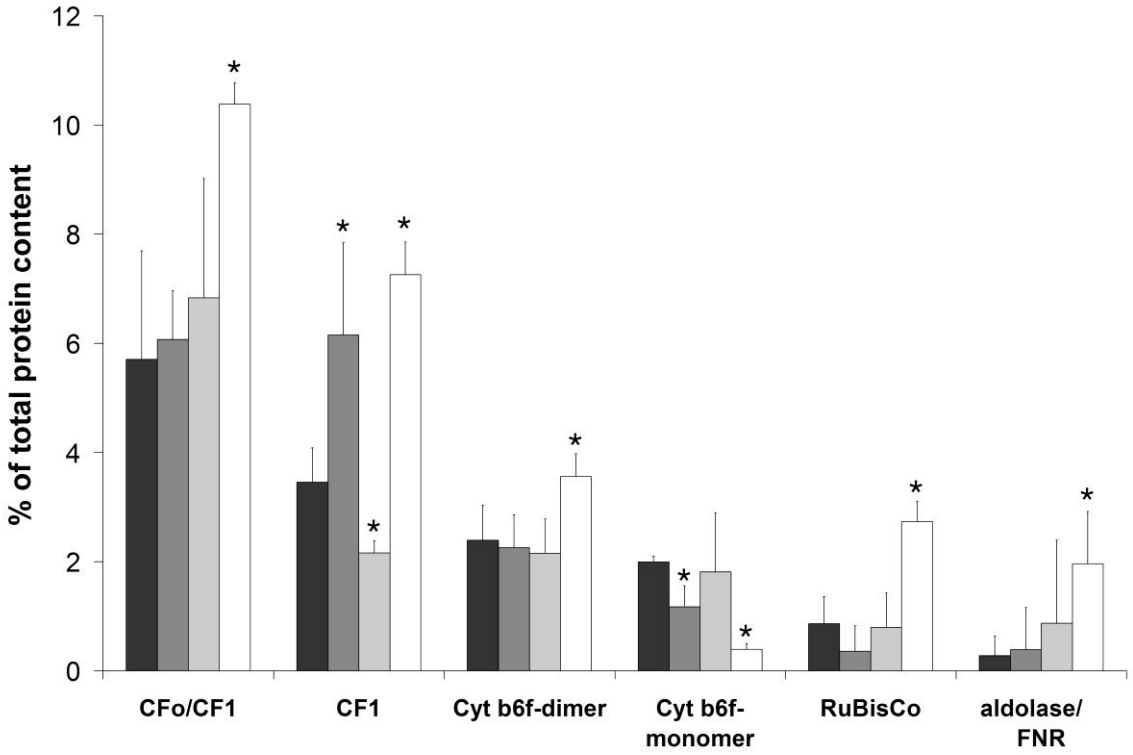
% of total protein content
12
10
8
6
4
2
0
CFo/CF1
CF1
Cyt b6f-dimer
Cyt b6f-monomer
RuBisCo
aldolase/FNR

Figure 5.

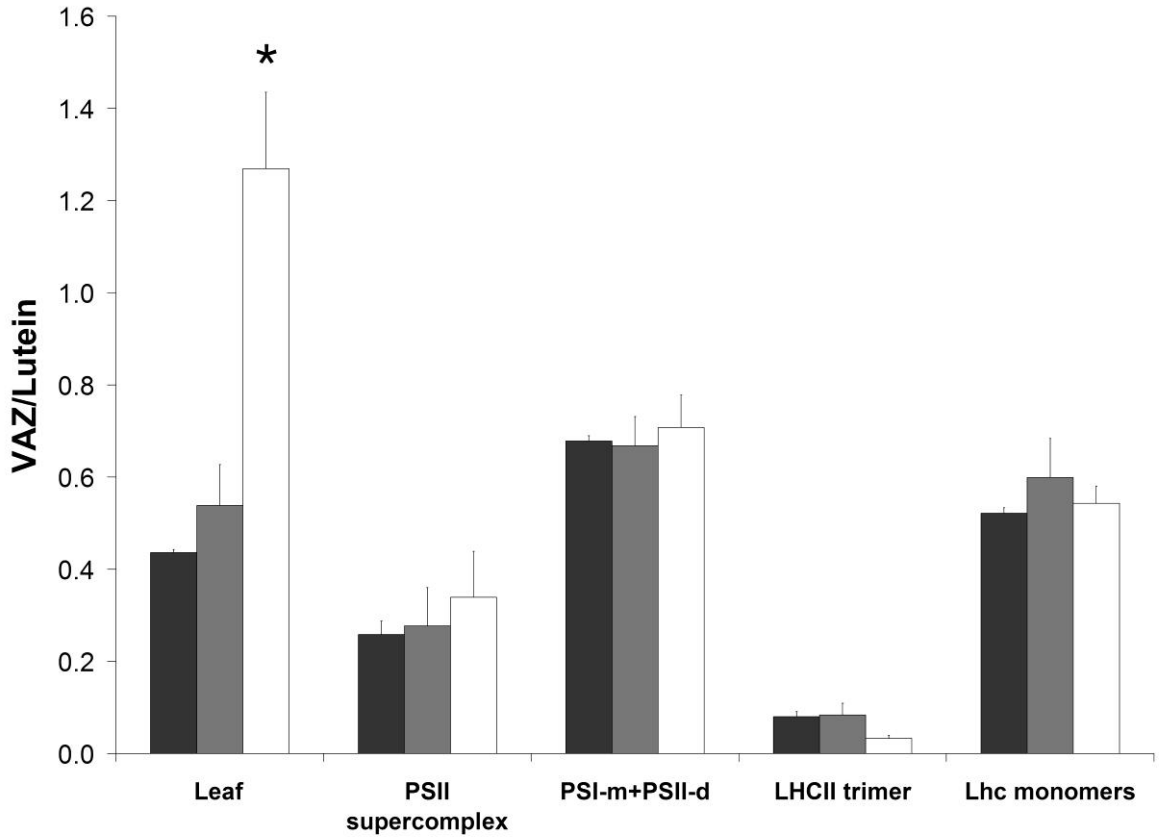
1.6
1.4
1.2
1.0
0.8
0.6
0.4
0.2
0.0
VAZ/Lutein
*
Leaf
PSII supercomplex
PSI-m+PSII-d
LHCII trimer
Lhc monomers

Figure 6.

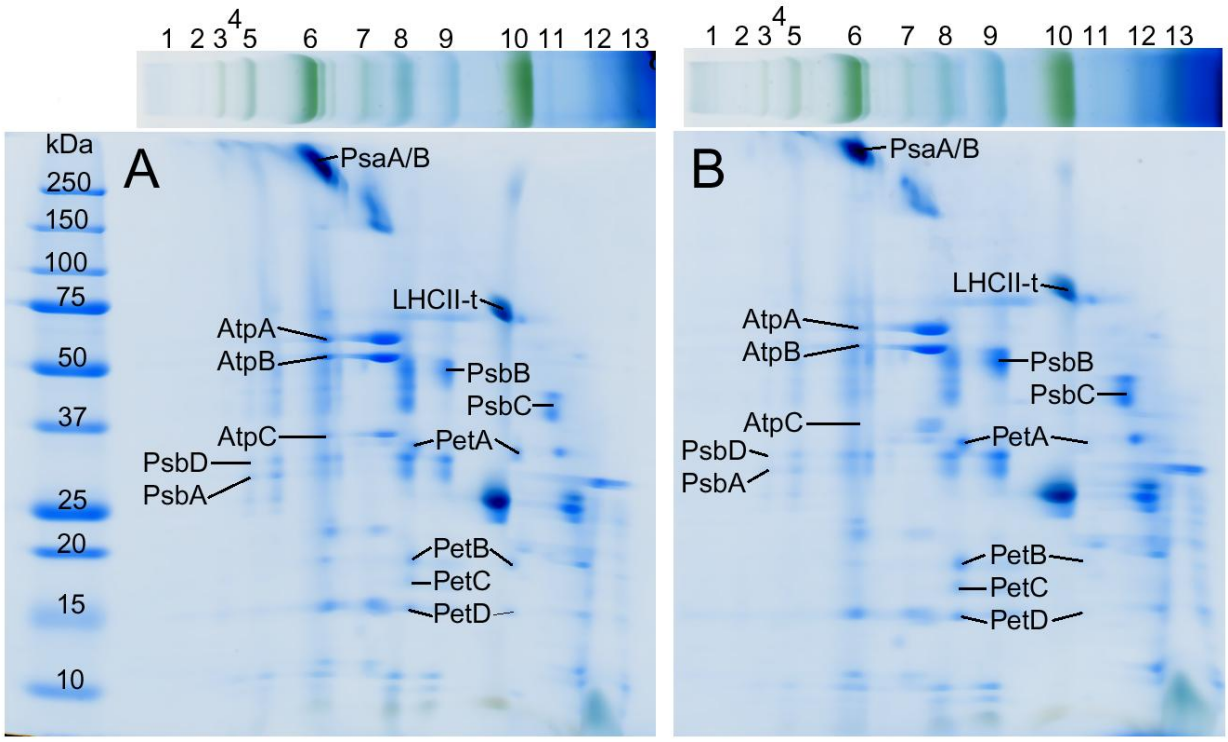

Supplementary figure 1.

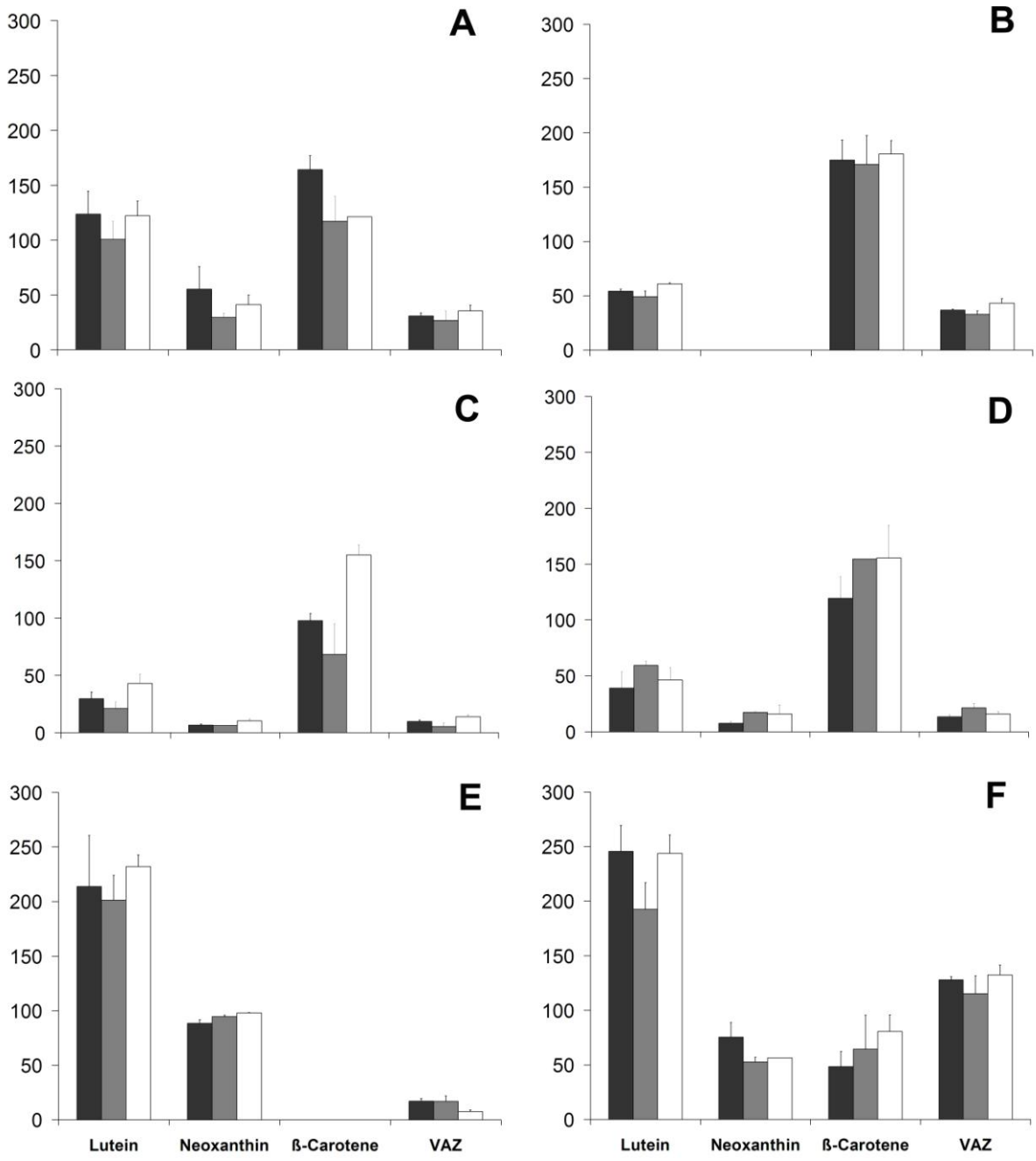

Supplementary figure 2.

Figure 1

Click here to download high resolution image

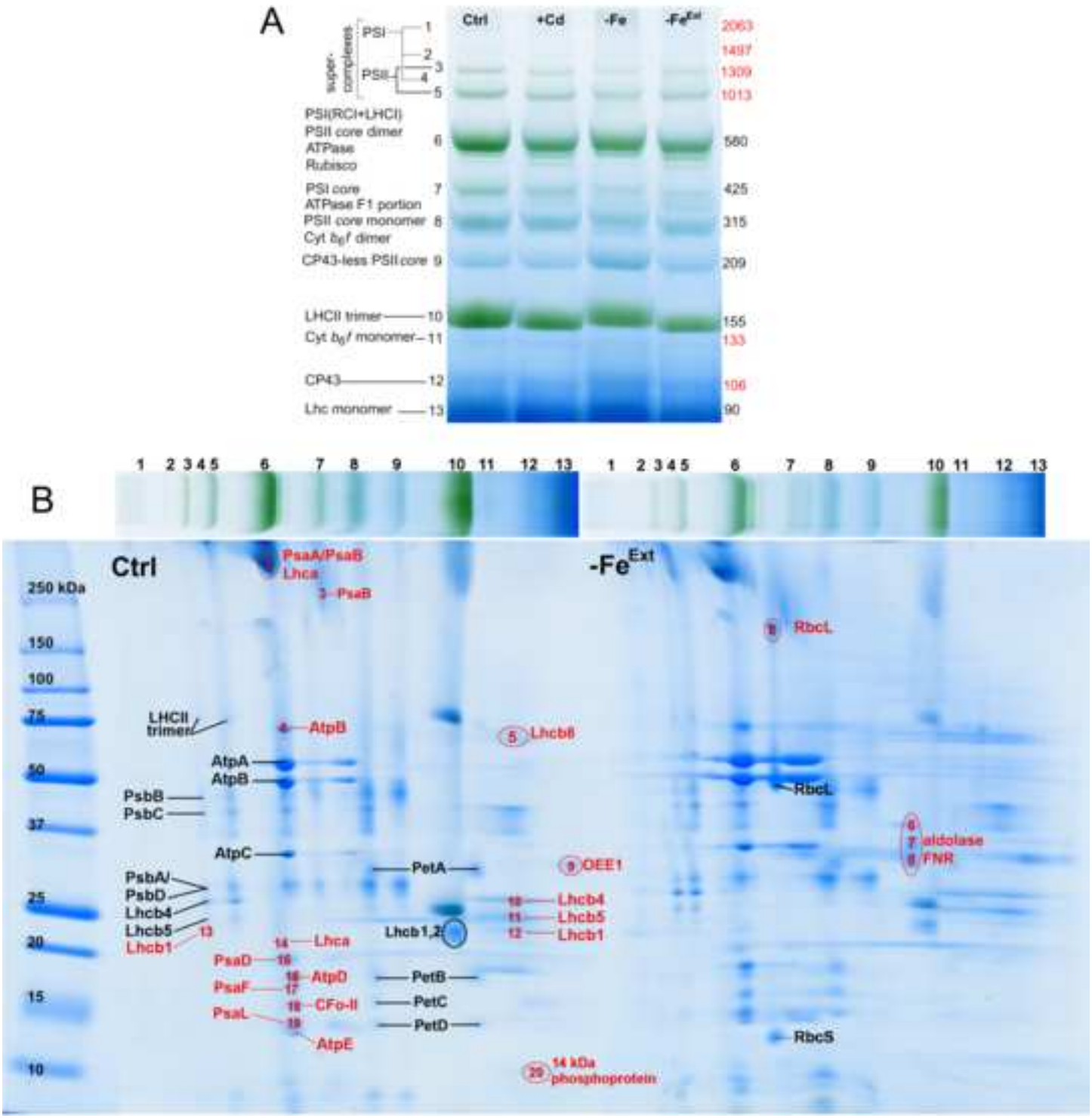

Figure 1

Click here to download high resolution image

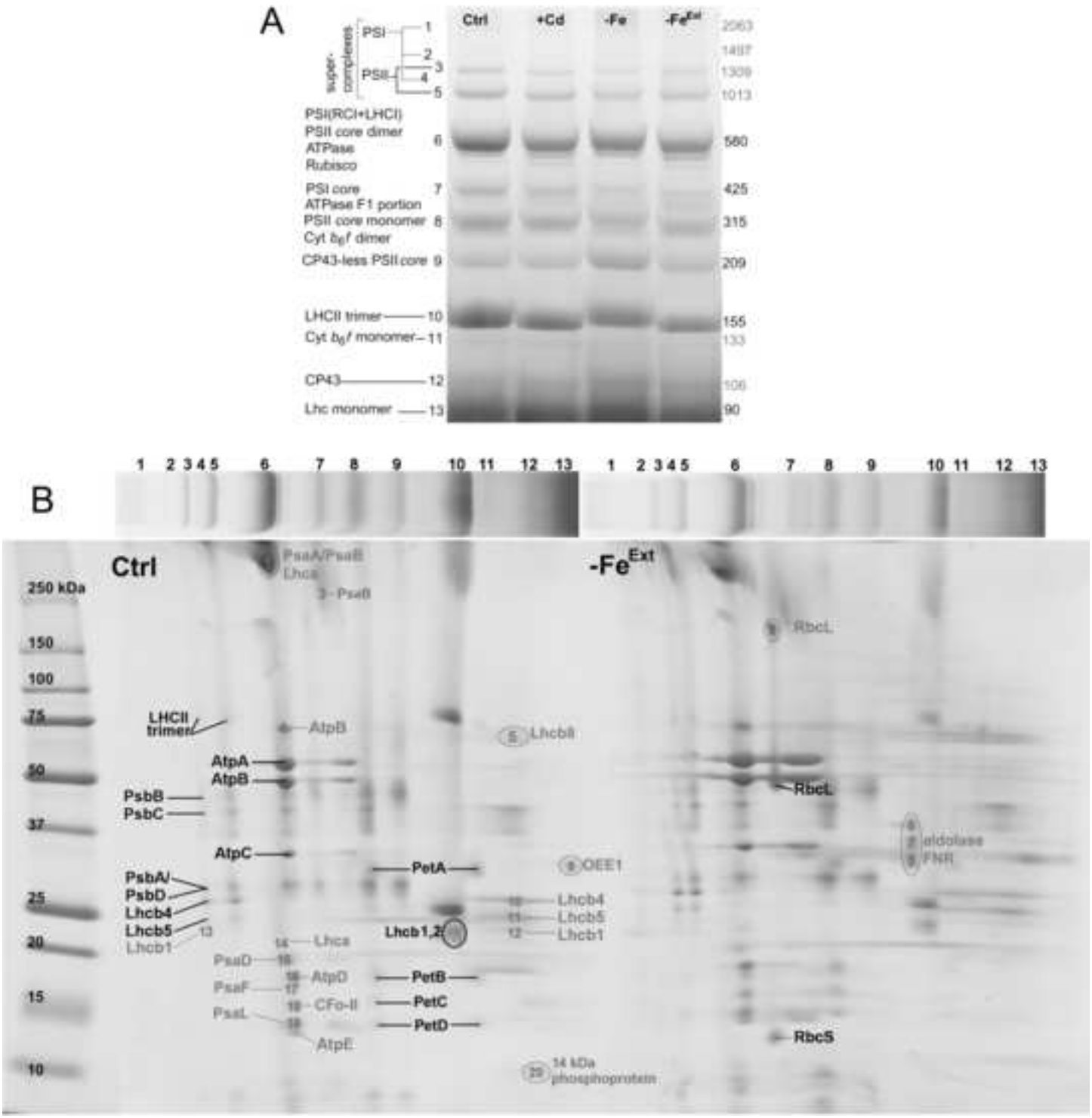

Figure 2

Click here to download high resolution image

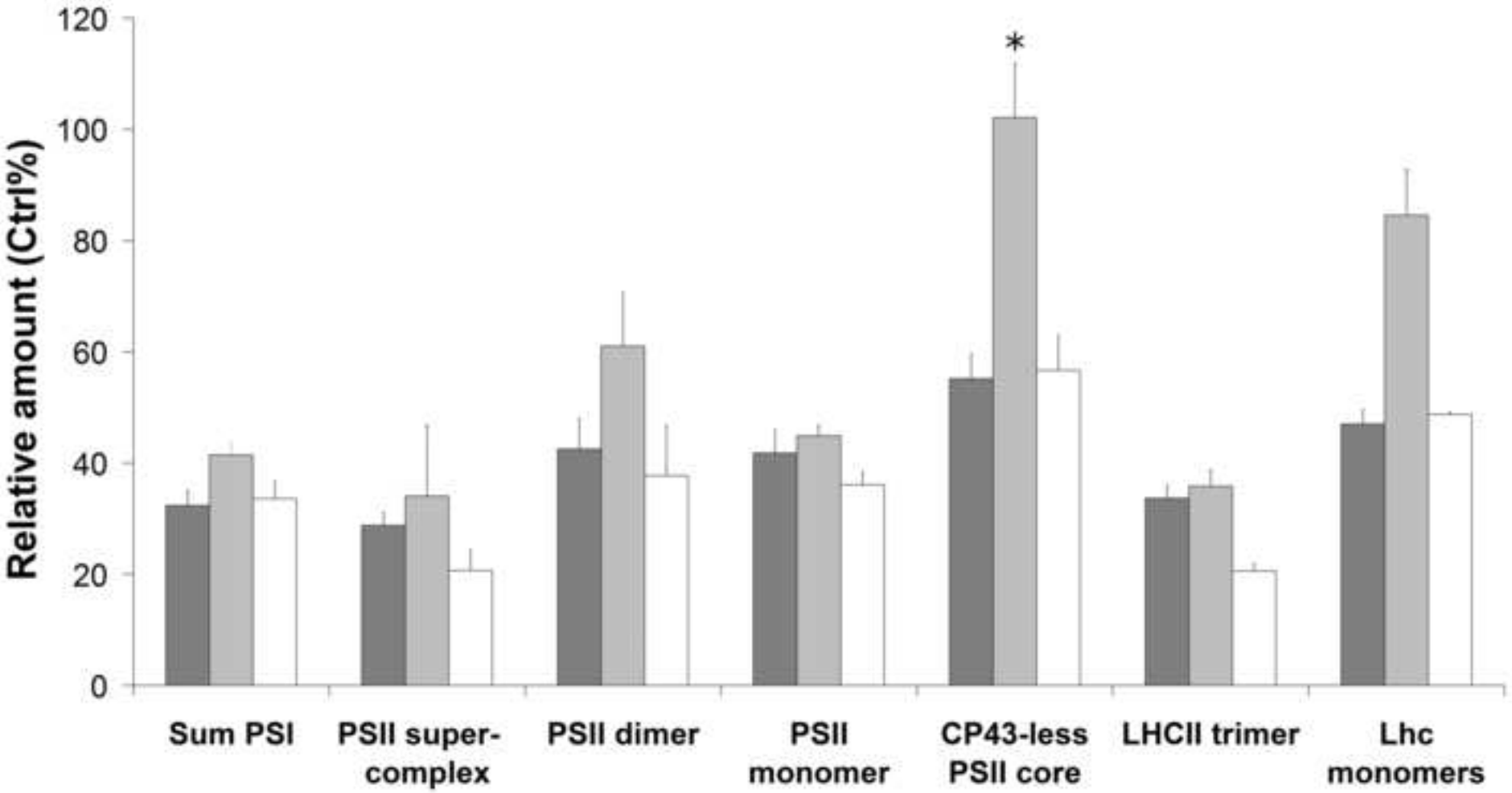

Figure 3

Click here to download high resolution image

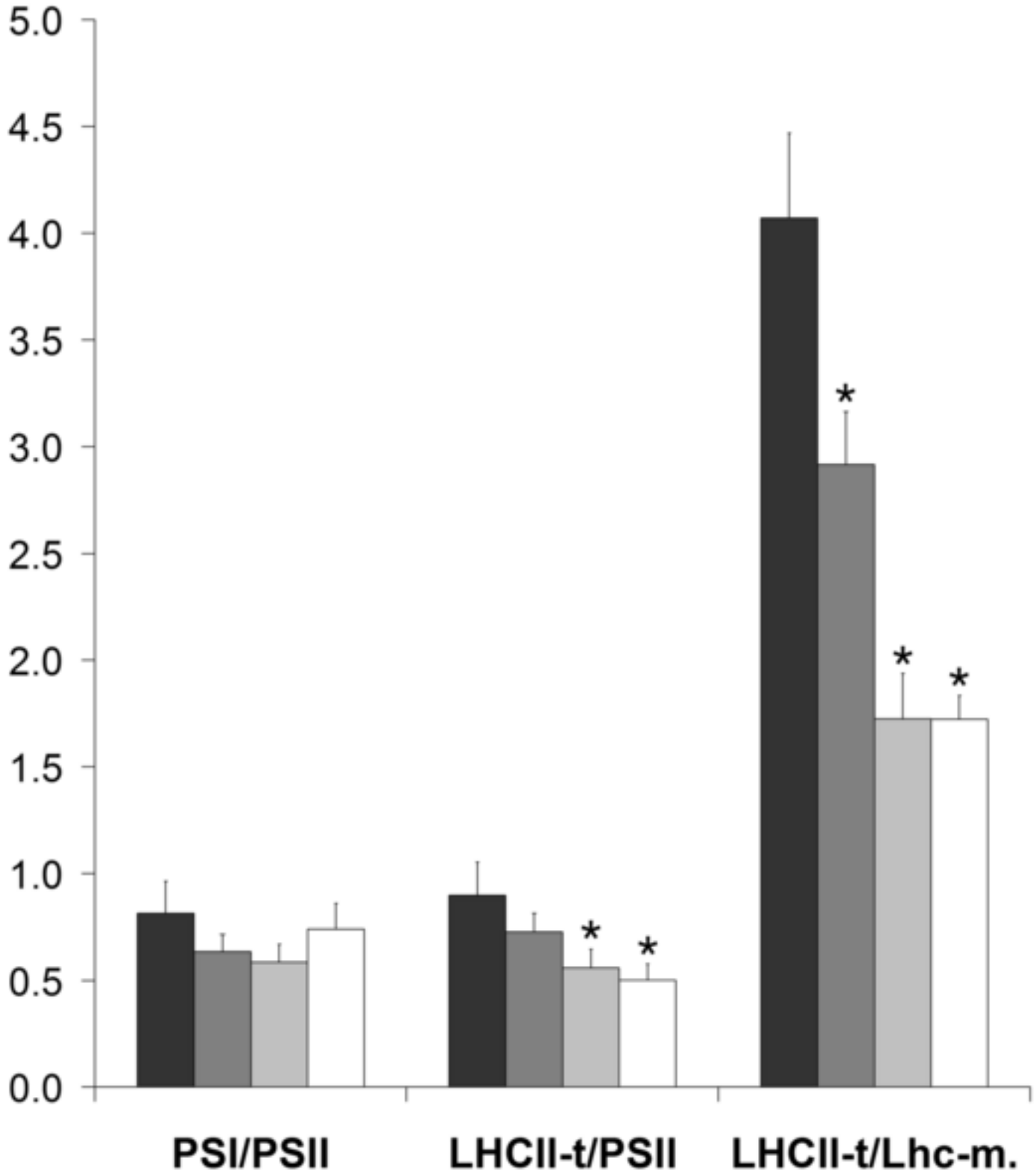

Figure 4

Click here to download high resolution image

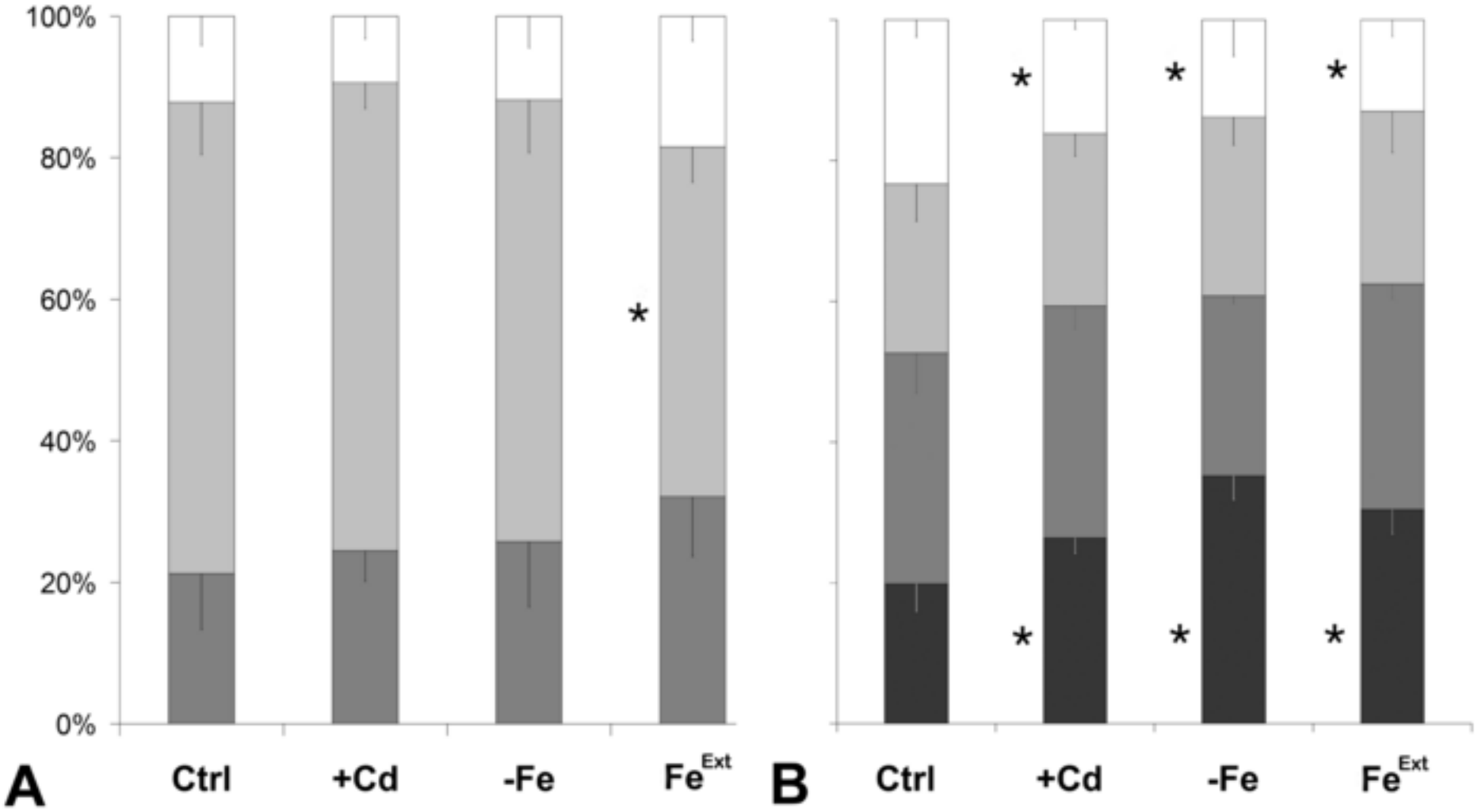

Figure 5

Click here to download high resolution image

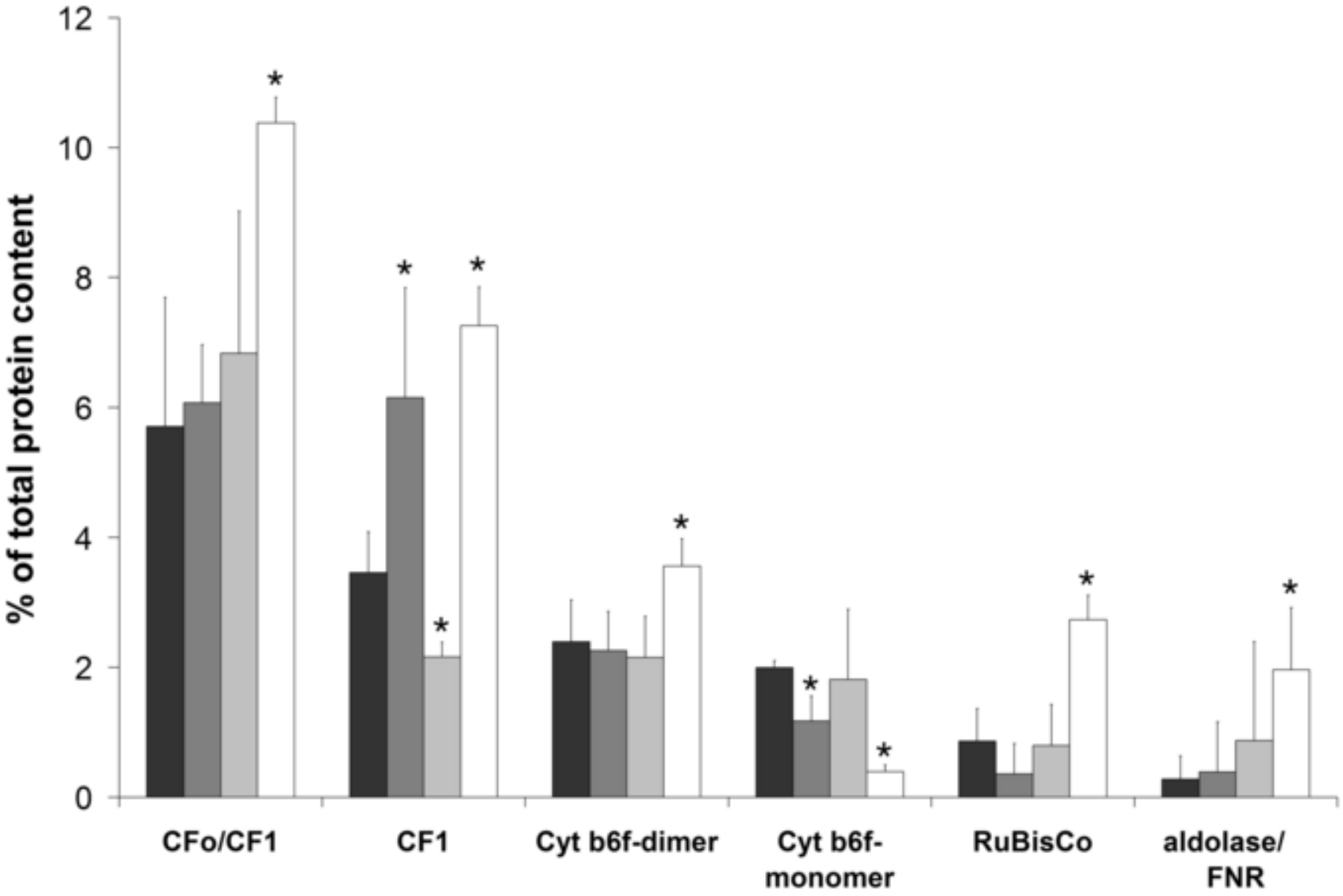

Figure 6

Click here to download high resolution image

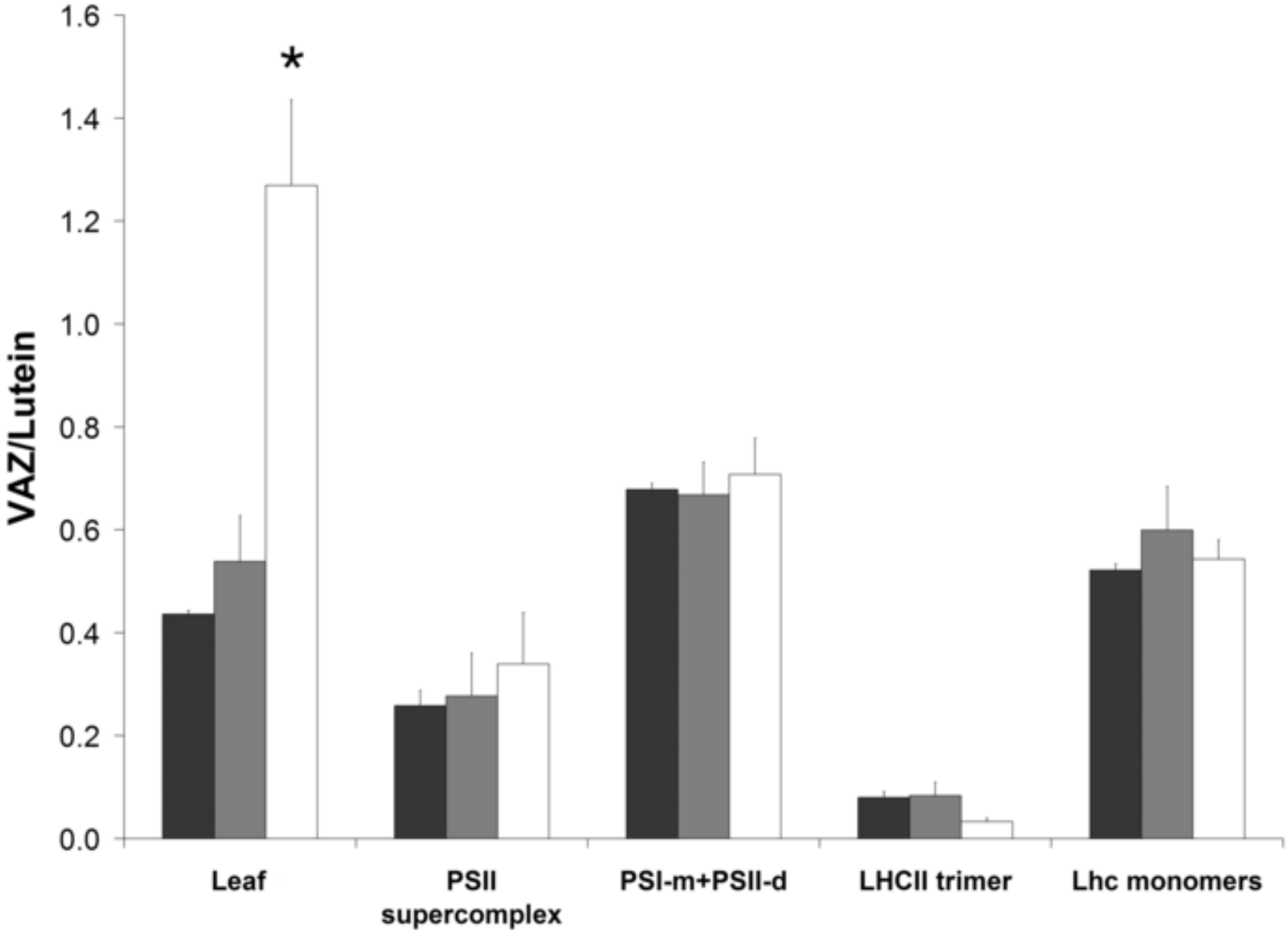

Fig 1. (A) 1-DE BN PAGE profiles of thylakoids isolated from leaves of control (Ctrl) and differently treated plants (see Table 1 for treatments). The molecular mass of the complexes was estimated (red numbers on the left) using data published by Fagioni et al. (*2009*) as standards (black numbers). Rubisco – ribulose 1,5-bisphosphate carboxylase-oxigenase. **(B)** 2-DE BN-SDS PAGE polypeptide patterns of thylakoids isolated from leaves of control and extremely iron deficient (-Fe^{Ext}) plants. Polypeptides identified on the basis of previous studies using similar gel systems are marked in black, whereas proteins identified in the present study by nano-HPLC combined with mass spectrometry are marked in red (Supplementary Table 1). FNR – ferredoxin-$NADP^+$ reductase.

Fig. 2. Changes in the amounts of different pigment-protein complexes in 1-DE BN PAGE gels of thylakoids isolated from leaves of plants affected by Cd toxicity and Fe deficiency (see Table 1 for treatments). Changes were estimated from the optical density of the bands and given as percentage of the control value. +Cd: dark grey; -Fe, light grey; -Fe^{Ext}, white. Sum PSI: bands *1*, *2*, *4*, *6*' and *7*; PSII super-complex: bands *3* and *5*; PSII dimer: band *6*"; PSII monomer: band *8*; CP43-less PSII core: band *9*; LHCII trimer: band *10*; Lhc monomers: band *13*. The optical density values for the controls (Fig. 1A) were as follows: Sum PSI, 539927±37245; PSII super-complex, 154748±16135; PSII dimer, 159367±34979; PSII monomer, 217804±38004; CP43-less PSII core, 131751±26066; LHCII trimer, 595840±9229; Lhc monomers, 146385±14154. In the case of band *6*, the contribution of the PSI monomer (*6'*) and the PSII dimer (*6"*) were estimated in the second dimension gel by comparing the density ratio of the CP47 apoprotein (PsbB) in band *6* with that of band *8*, which contains only PSII monomer. All the values differed significantly from the controls ($P < 0.05$) except the one signed: *****.

Fig. 3. Ratio of pigment-protein complexes estimated from the 1-DE BN PAGE gels of thylakoids from leaves of control plants and plants affected by Cd toxicity and Fe deficiency (see Table 1 for treatments). Control, black; +Cd, dark grey; -Fe, light grey; -Fe^{Ext}, white. LHCII-t – LHCII trimer, Lhc-m – Lhc monomer. The PSI/PSII, LHCII trimer/PSII and LHCII trimer/Lhc monomer ratios were estimated from the optical density of the bands as [bands *1*, *2*, *4*, *6'* and *7*]/[bands *3*, *5*, 6", *8* and *9*]), [band *10*]/[bands *3*, *5*, 6", *8* and *9*]) and [band *10*]/[band *13*]), respectively. *****values differing significantly from the controls ($P < 0.05$).

Fig. 4. Relative distribution of different PSI (A) and PSII (B) protein complexes in thylakoids from leaves of control plants and plants affected by Cd toxicity and Fe deficiency (see Table 1 for treatments), assessed from the 2-DE BN-SDS PAGE gels. The optical density values of all spots present in the second dimension of the different BN bands were used in the assessment, as follows: A) PSI supercomplex, white (bands *1*, *2* and *4*); PSI monomer, light grey (band *6'*); PSI core, dark grey (band *7*). B) PSII mega-/super-complexes, white (bands *3* and *5*); PSII dimer, light grey (band *6*"); PSII monomer, dark grey (band *8*); CP43-less PSII, black (band *9*). In the case of band *6* the contribution of the PSI monomer (*6'*) and the PSII dimer (*6"*) were estimated in the second dimension gel by comparing the density ratio of the CP47 apoprotein (PsbB) in band *6* with that of band *8*, which contains only PSII monomer. *values differing significantly from the control value ($P < 0.05$).

Fig. 5. Changes in the relative amount of other complexes and soluble proteins in thylakoids from leaves of control plants and plants affected by Cd toxicity and Fe deficiency (see Table 1 for treatments), assessed from the 2-DE BN-SDS PAGE gels. The optical density values of the corresponding spots were used to estimate the amounts of ATP synthase (bands *6* and *7*), Cyt b_6f complex (bands *8* and *11*), Rubisco (band *6* and zone at approximately 500 kD in the

1-DE BN gels) and a complex composed of aldolase and FNR (zone at approximately 180 kD in the 1-DE BN gels). Control (black), +Cd (dark grey), -Fe (light grey) and -Fe^{Ext} (white). *values differing significantly from the controls ($P < 0.05$).

Fig. 6. VAZ/lutein ratio in leaves and different 1-DE BN PAGE bands of thylakoids from leaves of control plants and plants affected by Cd toxicity and Fe deficiency. Control (black), +Cd (dark grey), -Fe^{Ext} (white). PSI-m: PSI monomer, PSII-d – PSII dimer, VAZ: violaxanthin-antheraxanthin-zeaxanthin. *****value differing significantly from the controls ($P < 0.05$).

Table 1

Table 1. Leaf chlorophyll (Chl) concentration and Chl *a* to Chl *b* ratio in control leaves and leaves affected by Cd toxicity and moderate and extreme Fe deficiency. +Cd: Cd treated, –Fe: moderately Fe deficient, -Fe^{Ext}: extremely Fe deficient. * values differing significantly from the controls ($P < 0.05$).

	Control	**+Cd**	**-Fe**	**-Fe^{Ext}**
Chl (µg cm^{-2})	53.1±3.9	*19.7±7.6**	25.7±1.9*	16.9±4.3*
Chl *a/b ratio*	3.3±0.1	3.9±0.2*	3.8±0.1*	*5.2±1.5**

Table 2. Photochemical efficiency and energy dissipation parameters in control leaves and leaves affected by Cd toxicity and extreme Fe deficiency (Fe^{Ext}; see Table 1 for treatments). Upper part: parameters for treated leaves are given in the shaded area (in italics) as percentages of those found in the controls. Lower part: proportions (in %) of the different mechanisms of energy dissipation. *values differing significantly from the controls (P <0.05).

	Control	**+Cd**	**-Fe^{Ext}**
F_v/F_m	0.84±*0.01*	*60.2±3.8**	*91.2±6.1**
$\Delta F/F_m'$	0.76±*0.02*	*66.7±3.8**	*87.1±6.1**
NPQ	0.22±*0.08*	*172.8±2.8**	*156.1±10.5**
Φ_{PSII}	73.7±*4.0*	30.4±*2.5**	55.9±*3.7**
Φ_{NF}	2.0±*1.0*	39.8±*0.2**	8.8±*0.6**
Φ_{NPQ}	2.6±*0.8*	8.3±*0.1**	2.6±*0.2*
$\Phi_{f,D}$	21.7±*1.5*	21.5±*1.3*	32.6±*2.2**

Table 3. Mineral composition of control leaves and leaves affected by Cd toxicity and Fe deficiency (see Table 1 for treatments). Cadmium concentrations in all samples and the rest of nutrient concentrations in the control are expressed in μg g^{-1} dry weight. Other nutrient concentrations in the treated leaves are given in the shaded area (in italics) as percentages of the values found in the controls. *values differing significantly from those of the controls ($P < 0.05$).

	Control	**+Cd**	**-Fe**	**-Fe^{Ext}**
Cd	0.9±0.2	633.0±82.3	1.2±0.2	1.2±0.3
K	36774±8337	*108.6±13.7*	*80.8±18.3*	*90.6±4.5*
Ca	18643±492	*144.8±4.0**	*124.3±7.6*	*148.7±3.9**
Mg	17556±6842	*54.3±1.1**	*53.1±20.7**	*37.7±14.7**
Fe	76.0±4.0	*56.1±3.0**	*89.4±4.7*	*24.9±2.7**
Mn	349.3±58.7	*34.2±11.6**	*50.4±8.5**	*15.7±2.6**
Zn	47.1±7.8	*88.5±8.9*	*118.4±19.5*	*127.1±21.0*

Figure 1

Click here to download high resolution image

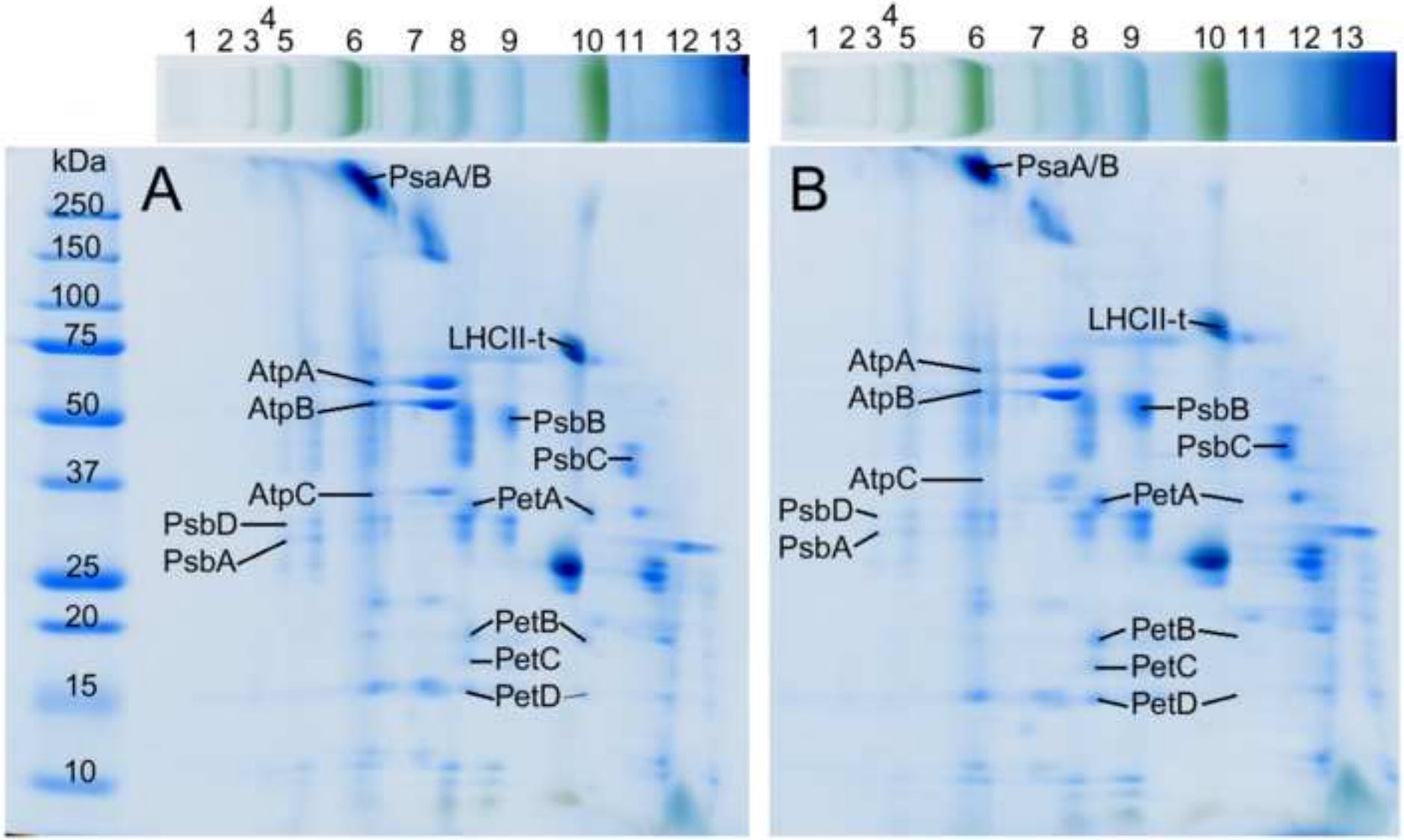

Figure 2

Click here to download high resolution image

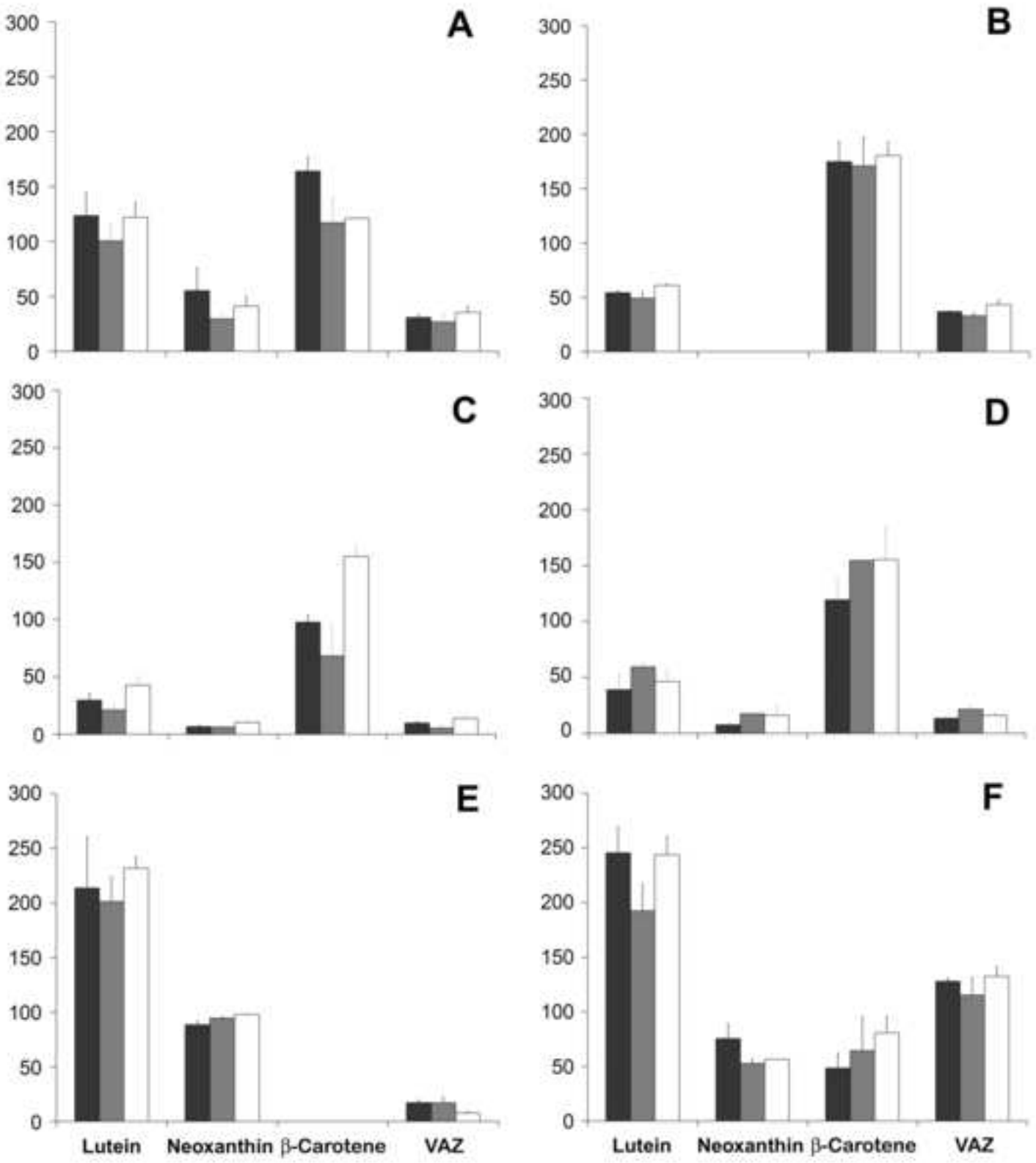

Table 1

Supplementary Table 1. Proteins identified in 2-DE BN-SDS PAGE gels. Positive identification was assigned with Mascot scores above the threshold level (P <0.05), at least 2 identified peptides (ion) with a score above homology and 10% sequence coverage. Protein score is –10*Log (P), where P is the probability that the observed match is a random event. Function was inferred from GO:P (biological process-P) annotation.

Spot number	Protein identification	Mass window (ppm)	MASCOT Score	Accesion No. NCBI/ EST	Mascot matches	No. of peptides	Sequence coverage (%)
	PSI core complex						
1	PsaB	100	156	gi|752032	4	2	3
	PsaA	100	82	gi|22091526	2	2	2
	PSI type III chlorophyll a/b-binding [Arabidopsis t.], Lhca3	100	163	gi|430947	3	2	10
3	PS I P700 chlorophyll a apoprotein A2, PsaB [Spinacia oleracea]	100	106	gi|11497524	2	2	3
15	Photosystem I reaction center subunit II, PsaD	75	390	gi|417544	34	6	28
17	Photosystem I reaction center subunit III, PsaF	100	130	gi|131187/ EG551670	3	3	10,5
19	Photosystem I subunit XI precursor , PsaL [Arabidopsis	75	65	gi|5738542	1	1	6

	thaliana]						
	Lhc proteins						
5	LHCB4.3 (light harvesting complex PSII), LHCB8 [Arabidopsis thaliana]	75	124	gi|15225630/BQ489041	2	2	21
10	Type I (26 kD) CP29 polypeptide [Solanum lycopersicum]	75	520	gi|19184/ BQ487648	10	7	42
11	LHCB5; chlorophyll binding, CP26 [Arabidopsis thaliana]	75	104	gi|15235028	2	2	9
12	LHCII type I CAB-40, LHCB1 (Nicotiana tabacum)	50	74	gi|19829	2	2	26
13	LHCII type I CAB-36, LHCB1 [Nicotiana tabacum]	75	84	gi|19827	2	1	8
14	PSI type III chlorophyll a/b-binding protein, LHCA3 [Arabidopsis thaliana]	75	155	gi|430947	5	3	14

	ATP synthase						
4	ATP synthase beta subunit [Anagallis arvensis]	75	260	gi|12004131	4	4	15
16	ATP synthase delta chain, chloroplast	100	369	gi|114584/ BQ487814	8	4	20
18	ATP synthase beta chain, chloroplast precursor (Subunit II)	100	64	gi|461595	1	1	4
	Membrane associated enzimes						
2	Rubisco Large Subunit	100	143	gi|118624224	4	3	9
9	33 kDa precursor protein of the OEC [Salicornia europaea]	75	363	gi|197691939	17	5	21
20	Thylakoid membrane phosphoprotein 14 kDa, chloroplast precursor, putative [Ricinus communis]	100	59	gi|255541776/ FG345112	2	1	4,6
6	fructose-bisphosphate aldolase, putative [Ricinus communis]	75	240	gi|255581400	17	5	16
7	Ferredoxin--NADP reductase, leaf isozyme, chloroplastic	75	300	gi|119905	9	5	15
8	fructose-bisphosphate aldolase, putative [Ricinus communis]	75	278	gi|255581400	44	6	19

Supplementary Fig. 1. 1-DE (upper horizontal gel bands) and 2-DE BN-SDS PAGE polypeptide patterns of thylakoids isolated from leaves of Cd-treated (**A**) and moderately Fe deficient (**B**) plants. Numbered lanes are: 1,2,4: PSI supercomplexes; 1,3,5: PSII supercomplexes; 6: PSI (RCI+LHCI), PSII *core* dimer, ATPase, Rubisco; 7: PSI *core*, ATPase CF1; 8: PSII *core* monomer, Cyt b_6f dimer; 9: CP43-less PSII core; 10: LHCII trimer; 11: Cyt b_6f monomer; 12: CP43; 13: Lhc monomer. Some of the characteristic polypeptides identified on the basis of previous studies using similar gel systems are marked (See Fig.1).

Supplementary Fig. 2. Carotenoid composition of BN bands belonging to thylakoids isolated from leaves of control plants and plants affected by Cd toxicity and Fe deficiency (see Table 1 for treatments). Control (black), +Cd (dark grey), $-Fe^{Ext}$ (white). VAZ: violaxantin-antheraxanthin-zeaxanthin. A: PSII mega/supercomplexes (bands *3*,*5*), B: PSI monomer and PSII dimer (band *6*), C: PSII *core* monomer (band *8*) D: CP43-less PSII *core* (band *9*), E: LHCII trimer (band *10*), F: Lhc monomers (band *13*).